

Copyright Warning & Restrictions

The copyright law of the United States (Title 17, United States Code) governs the making of photocopies or other reproductions of copyrighted material.

Under certain conditions specified in the law, libraries and archives are authorized to furnish a photocopy or other reproduction. One of these specified conditions is that the photocopy or reproduction is not to be “used for any purpose other than private study, scholarship, or research.” If a user makes a request for, or later uses, a photocopy or reproduction for purposes in excess of “fair use” that user may be liable for copyright infringement,

This institution reserves the right to refuse to accept a copying order if, in its judgment, fulfillment of the order would involve violation of copyright law.

Please Note: The author retains the copyright while the New Jersey Institute of Technology reserves the right to distribute this thesis or dissertation

Printing note: If you do not wish to print this page, then select “Pages from: first page # to: last page #” on the print dialog screen

The Van Houten library has removed some of the personal information and all signatures from the approval page and biographical sketches of theses and dissertations in order to protect the identity of NJIT graduates and faculty.

INFORMATION TO USERS

This reproduction was made from a copy of a document sent to us for microfilming. While the most advanced technology has been used to photograph and reproduce this document, the quality of the reproduction is heavily dependent upon the quality of the material submitted.

The following explanation of techniques is provided to help clarify markings or notations which may appear on this reproduction.

1. The sign or "target" for pages apparently lacking from the document photographed is "Missing Page(s)". If it was possible to obtain the missing page(s) or section, they are spliced into the film along with adjacent pages. This may have necessitated cutting through an image and duplicating adjacent pages to assure complete continuity.
2. When an image on the film is obliterated with a round black mark, it is an indication of either blurred copy because of movement during exposure, duplicate copy, or copyrighted materials that should not have been filmed. For blurred pages, a good image of the page can be found in the adjacent frame. If copyrighted materials were deleted, a target note will appear listing the pages in the adjacent frame.
3. When a map, drawing or chart, etc., is part of the material being photographed, a definite method of "sectioning" the material has been followed. It is customary to begin filming at the upper left hand corner of a large sheet and to continue from left to right in equal sections with small overlaps. If necessary, sectioning is continued again—beginning below the first row and continuing on until complete.
4. For illustrations that cannot be satisfactorily reproduced by xerographic means, photographic prints can be purchased at additional cost and inserted into your xerographic copy. These prints are available upon request from the Dissertations Customer Services Department.
5. Some pages in any document may have indistinct print. In all cases the best available copy has been filmed.

**University
Microfilms
International**

300 N. Zeeb Road
Ann Arbor, MI 48106

8517767

Chang, Shih-Hsin

KINETIC MODELING OF A LAMINAR-FLOW REACTOR

New Jersey Institute of Technology

D.ENG.SC. 1985

**University
Microfilms
International** 300 N. Zeeb Road, Ann Arbor, MI 48106

KINETIC MODELING OF A LAMINAR-FLOW REACTOR

By

Shih-Hsin Chang

Dissertation submitted to the Faculty of the Graduate School
of the New Jersey Institute of Technology in partial fulfillment
of the requirements for the degree of
Doctor of Engineering Science
1985

APPROVAL SHEET

Title of Thesis: Kinetic Modeling of a Laminar-Flow Reactor

Name of Candidate: Shih-Hsin Chang
Doctor of Engineering Science, 1985

Thesis and Abstract Approved:

_____ Date

Joseph W. Bozzelli
Associate Professor
Chemical Engineering
and Chemistry

_____ Date

_____ Date

_____ Date

_____ Date

ABSTRACT

Title of Thesis: Kinetic Modeling Of A Laminar-Flow Reactor

Shih-Hsin Chang, Doctor of Engineering Science, 1985

Thesis Directed by: Dr. Joseph W. Bozzelli
Associate Professor of Chemistry

The laminar-flow reactor considering radial dispersion for a species incurring first-order homogeneous (bulk) and heterogeneous (wall) chemical reactions was mathematically modeled. The equation was solved both analytically, and by the Crank-Nicolson finite-difference technique.

The response surface method was used to obtain the optimum values of the two rate constants. The optimum values interact because the wall and bulk reactions proceed in parallel. Varied reactor diameters serve to decouple the bulk and wall reactions to locate the true values of the rate constants.

Four dimensionless variables were defined and used to characterize the reacting system. In addition, their values were shown to determine the validity of the plug-flow model.

The reaction model was used in conjunction with experimental data to obtain the reaction rate constants for a system containing 1,1,1-trichloroethane and excess hydrogen, at temperatures ranging from 555 to 681 °C.

VITA

Name: Shih-Hsin Chang.

Degree and date to be conferred: D. Eng. Sc., 1985

Collegiate institutions attended	Dates	Degree	Date of degree
National Taipei Institute of Technology, Taipei, Taiwan	1966-71	Diploma Che. Eng.	1971
National Taiwan Institute of Technology, Taipei, Taiwan	1976-78	B.S. Ind. Mgt.	1978
Manhattan College Riverdale, NY	1979-80	M.S. Che. Eng.	1981

Major: Chemical Engineering.

Position held: Production Engineer, Taiwan Fertilizer Company
Nankang, Taiwan, 1975-79

To my family

ACKNOWLEDGEMENTS

I appreciate Dr. Joseph Bozzelli for his guidance. I shall remember his patience and kindness.

I express particular thanks to Dr. W.T. Wong, and my committee members, Drs. D. Hanesian, G. Lewandowski, A. Petroulas, R. Magee, and C.R. Huang who is currently on his sabbatical leave in China, for their opinions and comments.

TABLE OF CONTENTS

Chapter	Page
DEDICATION	ii
ACKNOWLEDGEMENTS	iii
TABLE OF CONTENTS	iv
LIST OF TABLE	vi
LIST OF FIGURES	vii
I. INTRODUCTION	1
II. THEORY	7
A. Continuity Equation	7
B. Determination of Eigenvalues	11
C. Numerical Solution	21
D. Optimization	32
E. Decoupling	36
F. Limiting Conditions	39
G. Validity of Plug-Flow Model	40
H. Bulk Reaction versus Wall Reaction	41
III. EXPERIMENTAL	43
A. Apparatus	43
B. Experimental Results	47
C. Kinetic Modeling of Laminar-Flow Reactor ...	50
D. Comparison of Analytical- with Numerical Solutions	55
E. Comparison with Plug-Flow Model	56
F. Correction of Rate Constants	60

Chapter	Page
G. Comparison of Rate Constants with Literature Values	64
H. Error Analysis	67
I. Mechanism	70
IV. CONCLUSIONS	71
A. Continuity Equation	71
B. Rate Constants	73
C. Thermal Decomposition of 1,1,1-Trichloroethane	75
NOTATIONS	76
APPENDIX 1. SOME PHYSICAL PROPERTIES OF HYDROGEN AND 1,1,1-TRICHLOROETHANE	78
APPENDIX 2. VAPOR PRESSURE OF 1,1,1-TRICHLOROETHANE ..	79
APPENDIX 3. CALCULATION OF RENOLDS NUMBER	80
APPENDIX 4. CALCULATION OF DIFFUSION COEFFICIENT	82
APPENDIX 5. LISTING OF COMPUTER PROGRAMS	83
A. Analytical Solution	83
B. Response Surface Method for k_D & k_W Estimations	90
APPENDIX 6. MECHANISTIC ANALYSIS	103
SELECTED BIBLOGRAPHY	107

LIST OF TABLES

Table	Page
1. Comparison between w_{true} and w_{estimate}	17
2. Eigenvalues and function coefficients	19
3. Comparison of analytical and numerical solutions with experimental results	23
4. k_b and k_w with temperature	53
5. k_{expt} (1/sec) as calculated using the plug-flow model	57
6. Comparison of k_b and k_w --- laminar- versus plug- flow model	59
7. Estimated precision with 95% confidence interval	68

LIST OF FIGURES

Figure	Page
1. The typical numerical behavior of $f(w)$	12
2. The continuous curve is constituted by an infinite number of pairs of the coupled optimum $\log k_b$ and k_w	33
3. Response surface represents SSR versus $\log k_b$ and $\log k_w$	34
4. The intersection of two curves characterized by diameter gives the true values of $\log k_b$ and $\log k_w$	37
5. Experimental apparatus	44
6. Concentration-time curves for the pyrolysis of 1,1,1-trichloroethane in the presence of hydrogen	48
7. Concentration-time curves for the pyrolysis of 1,1,1-trichloroethane in the presence of hydrogen	49
8. The intersection of curves in each set gives the true $\log k_b$ and $\log k_w$ for the pyrolysis of CH_3CCl_3 in H_2	51
9. The center of gravity of the triangle gives the true values of k_b and k_w	52
10. Dependencies of rate constants on temperature ..	54
11. k_b and k_w from the plug-flow model	58

Figure	Page
12. k_b and k_w at 954 °K are corrected by extrapolating the straight $\log k_b - \log k_w$ line to the 0.4 cm-curve at 954 °K	61
13. The values of k_b and k_w at 954 °K are corrected	62
14. Comparision with literature values	66

I. INTRODUCTION

The decomposition and/or conversion of chlorinated hydrocarbon such as poly(vinyl chloride) (PVC), chlorinated dry cleaning solvents, dichlorodiphenyl-trichloroethane (DDT) and pesticides, to desirable hydrogen chloride (HCl) and hydrocarbons in an hydrogen atmosphere at high temperatures is a promising approach to resolve the problems related to incomplete combustion or destruction of undesirable halocarbon species in addition to likely formation of valuable hydrocarbon feed-stock. Chuang (1982) and Mahmood (1985) have extensively studied the reactions of chloroform, 1,1,2-trichloroethane and 1,1-dichloroethane with hydrogen in isothermal tubular-flow reactors at temperatures ranging from 500 to 1100 °C. Mahmood's data showed, e.g., that chlorocarbon in hydrogen could be completely converted to acetylene, ethylene, methane and benzene at a temperature of 900 °C.

Thermal decomposition, of gaseous chlorinated hydrocarbons as well as many other organic substances, at high temperature occurs via two mechanisms - heterogeneous (wall or surface) and homogeneous (bulk) reactions (Mulcahy, 1973). The overall concentration change of the reactant is consequently the sum or resultant of these two mechanisms. The relative importance of the wall over the bulk reaction

is not a function of temperature alone. It also depends on the surface-to-volume ratio of the reactor employed; thus, the relative contribution of surface reaction will be more important in a smaller reactor than it is in a larger reactor. On the other hand, the bulk reaction will be more important in a larger reactor. One has to separate the individual rate effects from the experimental data on these two combined reactions, if they are of similar importance, in order to determine the specific rate constants.

The continuity equation of the reacting system should first be set up and analyzed before we attempt to accurately extract the individual values of the wall, k_w , and the bulk, k_b , rate constants from the experimental data. In an experimental-scale tubular-flow reactor, radial diffusion is often a significant consideration due to reactor size and wall removal effect, while the axial dispersion can be negligible if the gaseous velocity is sufficiently large (Levenspiel, 1972; Howard, 1979). The laminar-flow pattern is in addition usual, and is assumed under steady-state operation here. Furthermore, the condition on the reaction to follow first-order kinetics is also helpful for ease of mathematical treatment.

The governing equation formulated with these considerations can be solved, and Lauwerier (1959) obtained the analytical solution to this governing equation subject

to no wall removal reaction. Wissler and Schechter (1961), using the solution of Lauwerier, carried out numerical calculations, with results in good agreement to those from numerical method of Cleland and Wilhelm (1956). Black, Wise, Schechter and Sharpless (1974) took the wall reaction into account in dealing with de-excitation of nitrogen on a variety of different solid surfaces; but their system with only wall reaction occurring, excluded bulk reaction.

There are two research publications which, in solving the governing continuity equation, considered both the bulk and the wall reactions. Poirier and Carr (1971) employed a finite difference method to solve the continuity equations for first- and second- order chemical reactions. The second study was by Orgen (1975), who solved the equation in infinite series. He then, without employing the orthogonality relationship of the eigenfunctions to obtain function coefficients, directed his work toward analysis of the deviation between a laminar-flow system and the plug-flow model.

The purpose of this paper is to extend the model of Lauwerier to include the wall reaction, and provide helpful aspects to computer programming by showing some properties of the function by which eigenvalues are evaluated for the analytical solution. The governing equation is in addition solved using Crank-Nicolson finite-difference method

(Lapidus, 1967) for comparison purpose. The results show that the accuracy of the numerical solution is comparable to the analytical and that the numerical method is more computer time efficient. The numerical method is employed when the equation of continuity is solved repeatedly to get the optimum values of k_b and k_w .

Secondly, we apply the response surface method (Box and Wilson, 1951; Box, Hunter and Hunter, 1978) to evaluate the optimum values of k_b and k_w , and elucidate a general relationship on the response (the sum of the squares of the residuals between the calculated and experimental concentration data) versus its factors (k_b and k_w), the rate constants.

The bulk reaction coupled with the wall reaction forms a system of two parallel reactions, in which we can only determine the ratio of k_b over k_w (Levenspiel, 1972). Thus, we will instead obtain an infinite number of optimum pairs of k_b and k_w , as we try to evaluate them from the experimental data. Poirier and Carr, as mentioned above, extracted with the given k_w the k_b from the overall (experimental) rate constant, k_{expt} , in dealing with the atomic hydrogen-nitrogen dioxide reaction system, while the k_w of the heterogeneous recombination of oxygen atom was, in the Smith, Krieger and Herzog's work (1980), calculated from the overall rate equation with values of other kinetic

parameters given. In the evaluation of one rate constant where the other is given, one should be aware that the known value may not always be applicable to the particular experimental conditions. The third step in our research is, therefore, to decouple the interaction between these two rate constants and simultaneously get their true values. We also show the limiting conditions under which either k_b or k_w may be determined alone.

Finally, the chemical reaction system which we are interested in is 1,1,1-trichloroethane in excess hydrogen, whose thermal decomposition (500 - 1000 °C) has not been previously studied. There are, however, two relevant works. Barton and Onyon (1950) studied the pyrolysis of pure 1,1,1-trichloroethane in batch reactors at temperatures from 635 to 707 °K and pressures from 10 to 120 mmHg. They found that the decomposition rate in the packed reactor was slower than that in the empty reactor. They proposed the packed reactor has a larger surface-to-volume ratio so the recombination of some radicals to terminate the chain reactions occurred at a faster rate and slowed the overall process. They reported that the pyrolysis of 1,1,1-trichloroethane was unimolecular and obeyed first-order kinetics.

Benson and Spokes (1967), in addition, employed the very low pressure techniques (so that the tubular-flow reactor was operating at gas flow rates from 10^{15} to 10^{16}

molecules/sec and most of the collisions made by reactant molecules were with wall rather than with other gas molecules) to estimate the homogeneous rate constant of the thermal decomposition of 1,1,1-trichloroethane at high pressure limit. Our kinetic results are compared and in agreement with both of these previous studies. We also propose a detailed mechanism for this global reaction.

The plug-flow model concentration profile for our reaction system is shown to be reasonable, and a comparison of the plug-flow model with the more rigorous laminar-flow model is included.

II. THEORY

A. CONTINUITY EQUATION

The model considers that a laminar fluid of constant density flows through a tubular reactor. A species of low concentration is well mixed, moving with the fluid and is undergoing first-order chemical reaction. Radial dispersion serves to compensate the concentration gradient created by the parabolic profile of velocity and to balance the heterogeneous removal reaction at the wall of the reactor. The axial dispersion is negligible due to the high Peclet number. This model is accurately represented by the partial differential equation in its dimensionless form

$$4(1 - u^2) \frac{\partial c'}{\partial v} = \frac{1}{u} \frac{\partial}{\partial u} \left(u \frac{\partial c'}{\partial u} \right) - 4\alpha c' \quad (1)$$

with the boundary conditions

1. $c' = 1$ at $v = 0$,
2. $c' = \text{finite}$ at $u = 0$,
3. $3 - \frac{\partial c'}{\partial u} = 2\beta c'$ at $u = 1$.

where

$$u = \frac{r}{R}, \quad v = \frac{4Dz}{V_0 R^2}, \quad c' = \frac{C}{C_0},$$

$$\alpha = \frac{k_b R^2}{4D}, \quad \text{and} \quad \beta = \frac{k_w R}{2D}$$

$2/R$ is the surface-to-volume ratio of a cylinder. It is

theoretically sound and numerically consistent to define α and β in this way. We can see that α represents the ratio of the characteristic homogeneous removal rate constant, k_b , to the characteristic diffusion rate constant, $D/(R/2)^2$, and β , the characteristic heterogeneous removal rate constant, $(2/R)k_w$, to $D/(R/2)^2$. The radial concentration profile therefore flattens out as both α and β get smaller; the criterion on which the concentration change of the reacting species may well be approximated by the plug-flow model considering the radial dispersion is $(\alpha, \beta) \leq (0.25, 0.50)$ (Smith, Krieger and Herzog, 1980). We would, moreover, instead of defining $\alpha = D/(k_b R^2)$, avoid in determination of the rate constants by optimization technique the case of α becoming infinite.

We let (Lauwerier, 1959)

$$C'(u, v) = R'(u)Z'(v) \quad (2)$$

We then have two ordinary differential equations:

$$\frac{d^2 R'}{du^2} + \frac{1}{u} \frac{dR'}{du} + 4[w(1 - u^2) - \alpha]R' = 0 \quad (3)$$

$$\frac{dZ'}{dv} = -wZ' \quad (4)$$

where w is a positive, real constant of separation.

Eq. 3 has a regular singularity at $u = 0$ and coefficients regular for all $u \neq 0$; it can be integrated in terms of confluent hypergeometric function (Slater, 1960).

The solution of Eq. 4 is of exponential function.

The particular solution of Eq. 1 in its complete form is

$$C'(u, v) = \sum_{n=1}^{\infty} B_n \text{Exp}(-w_n v) \text{Exp}(-w_n^{1/2} u^2) {}_1F_1[a_n; 1; 2w_n^{1/2} u^2] \quad (5)$$

where B_n is coefficient of function, $a_n = \frac{1}{2} - \frac{w_n - \alpha}{2w_n^{1/2}}$ and

$${}_1F_1[a; b; x] = \sum_{r=0}^{\infty} \frac{(a)_r x^r}{(b)_r r!}, \text{ in general.}$$

Determination of the eigenvalue w results from satisfying the boundary condition at $u = 1$. It requires solving Eq. 6 for its roots:

$$f(w) = (\beta - w^{1/2}) {}_1F_1[a; 1; 2w^{1/2}] + 2aw^{1/2} {}_1F_1[a+1; 2; 2w^{1/2}] \quad (6)$$

The determination of coefficient B results from satisfying the boundary condition at $v = 0$, and it yields the expression:

$$B_n = \frac{\int_0^1 u(1 - u^2) \text{Exp}(-w_n^{1/2} u^2) {}_1F_1[a_n; 1; 2w_n^{1/2} u^2] du}{\int_0^1 u(1 - u^2) \{ \text{Exp}(-w_n^{1/2} u^2) {}_1F_1[a_n; 1; 2w_n^{1/2} u^2] \}^2 du} \quad (7-1)$$

$$\begin{aligned}
& \sum_{i=0}^{\infty} \frac{(C_1)_i (2w_n^{1/2})^{i+1}}{(i+1)(i+2)} \\
= & \frac{\sum_{i=0}^{\infty} \frac{(C_2)_i (2w_n^{1/2})^{i+1}}{(i+1)(i+2)}}{\quad} \quad (7-2)
\end{aligned}$$

where

$$(C_1)_i = \sum_{j=0}^i \left[\left(\frac{-1}{2} \right)^j \frac{(a)_{(i-j)}}{j! (b)_{(i-j)} (i-j)!} \right]$$

and

$$(C_2)_i = \sum_{j=0}^i \left\{ \frac{(-1)^j}{j!} \sum_{k=0}^{i-j} \left[\frac{(a)_k (a)_{(i-j-k)}}{(b)_k (b)_{(i-j-k)} k! (i-j-k)!} \right] \right\}$$

The following orthogonal relationship was applied in order to obtain Eq. 7-1.

$$\int_0^1 \{ u(1-u^2) \text{Exp}(-w_m^{1/2} u^2) {}_1F_1[a_m; 1; 2w_m^{1/2} u^2] \text{Exp}(-w_n^{1/2} u^2) {}_1F_1[a_n; 1; 2w_n^{1/2} u^2] \} du = 0, \quad m \neq n \quad (8)$$

B. DETERMINATION OF EIGENVALUES

It is better to look at the general numerical behavior of the function $f(w)$ in Eq. 6 before we determine the roots of $f(w)$. We rewrite $f(w)$ in a different form by first expressing its two confluent hypergeometric functions in series, and distributing each $2w^{1/2}$ in powers among each of $(a)_r$. The distribution is in general

$$(a + r - 1)(2w^{1/2}) = (2r - 1) w^{1/2} - w + \alpha$$

Then Eq. 6 becomes

$$f(w) = (\beta - w^{1/2}) \left\{ 1 + \sum_{n=1}^{\infty} \frac{\prod_{r=1}^n [(2r-1)w^{1/2} - w + \alpha]}{n! n!} \right\} +$$

$$(w^{1/2} - w + \alpha) \left\{ 1 + \sum_{n=1}^{\infty} \frac{\prod_{r=1}^n [(2r+1)w^{1/2} - w + \alpha]}{(n+1)! n!} \right\} \quad (9)$$

We have at $w = 0$

$$f(0) = \beta \left(1 + \alpha + \frac{\alpha^2}{4} + \dots + \frac{\alpha^n}{n! n!} + \dots \right) +$$

$$\alpha \left(1 + \frac{\alpha}{2} + \frac{\alpha^2}{12} + \dots + \frac{\alpha^n}{(n+1)! n!} + \dots \right) \quad (10)$$

We can therefore depict the typical numerical behavior of $f(w)$, starting at $[0, f(0)]$, as shown in Fig. 1. $f(w)$ is an oscillating function; both of its wavelenghtes and amplitudes gradually grow as w increases. The Newton-Raphson method appears to be attractive for evaluating eigenvalues because $f(w)$ is so steep. However, there are several key

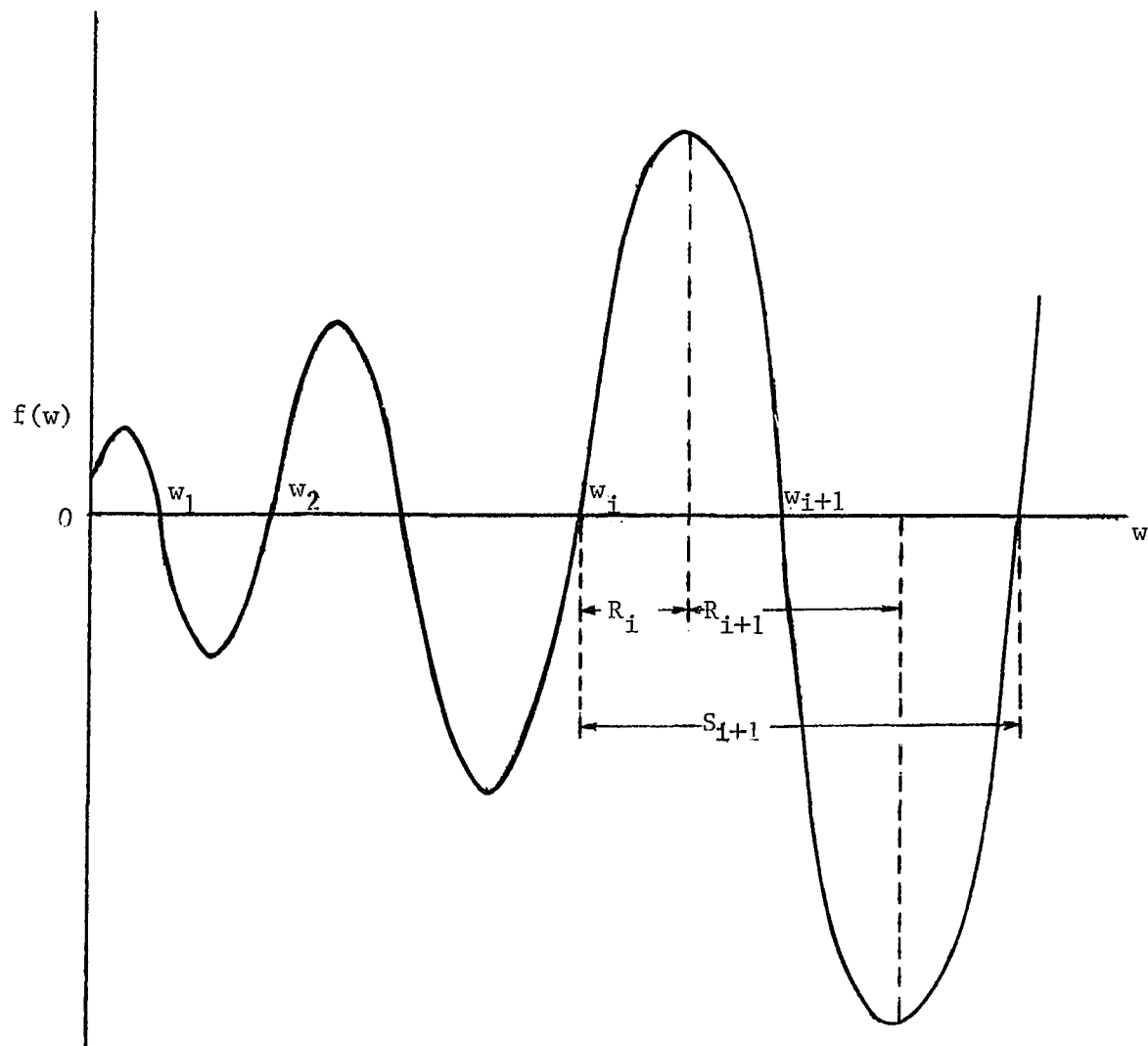


Fig. 1: The typical numerical behavior of $f(w)$.

elements important to a successful evaluation program.

These elements are:

1. The derivative of $f(w)$ with respect to w .
2. Initial value for the first eigenvalue, w_1 .
3. Initial value for the next eigenvalue.
4. Restriction on the correction value during iteration.

and they are discussed as follows:

Element 1: the derivative of ${}_1F_1[a;b;x]$ with respect to w is needed in using Newton-Raphson method to estimate w . Here, both a and x depend of w , while b is a constant. The derivative of concern is

$$\frac{d{}_1F_1}{dw} = \frac{\partial {}_1F_1}{\partial a} \frac{da}{dw} + \frac{\partial {}_1F_1}{\partial x} \frac{dx}{dw} \quad (11)$$

where

$$\frac{\partial {}_1F_1}{\partial a} = \sum_{r=1}^{\infty} \frac{(a)_r x^r}{(b)_r r!} \sum_{n=1}^r \frac{1}{(a+n-1)} \quad (12)$$

and

$$\frac{\partial {}_1F_1}{\partial x} = \frac{a+1}{b+1} {}_1F_1[a+1;b+1;x] \quad (13)$$

A special treatment of Eq. 11 is necessary if

$$a + r - 1 = 0 \quad (14)$$

Let M be the absolute value of a . The result is

$$\frac{\partial {}_1F_1}{\partial a} = \sum_{r=1}^M \frac{(a)_r x^r}{(b)_r r!} \sum_{n=1}^r \frac{1}{(a+n-1)} + \sum_{t=M+1}^{\infty} \frac{(a)_t^M x^t}{(b)_t t!} \quad (15)$$

where $(a)_t^M = a(a+1)\dots(a+M-1)(a+M+1)\dots(a+t-2)(a+t-1)$.

Element 2: The first eigenvalue w_1 may go into the negative domain if the initial guess is less than the true value. The following relationship is valid (Lauwerier, 1959)

$$w_1 = 2\alpha - \frac{\alpha^2}{12} + \frac{\alpha^3}{60} + O(\alpha^4) \quad (16)$$

for small α and no wall reaction where the $O(\alpha^4)$ is the fourth order remainder. In the case of both α and β being small the plug-flow approximation is valid. Kaufman (1961) showed that

$$k_{\text{expt}} = k_b + \frac{2}{R} k_w \quad (17)$$

Assuming that

$$\alpha_{\text{expt}} = \frac{k_{\text{expt}} R^2}{4D} \quad (18)$$

$$\alpha_{\text{expt}} = \alpha + \beta \quad (19)$$

follows immediately. Computer simulation showed that α and β are exchangeable as (α, β) is less than $(0.01, 0.01)$. The following expression, therefore, provides a good initial guess for the first eigenvalue, w_1 :

$$w_1 = 2(\alpha + \beta) - \frac{(\alpha + \beta)^2}{12} + \epsilon \quad (20)$$

where the $\epsilon \rightarrow 0^+$ is added to prevent w_1 from becoming zero or negative, even though the true value of w_1 is zero when both α and β are zero.

In the case as α and/or β are large, it is convenient

to discuss the following two subcases:

1. $\beta = 0$ and $\alpha \rightarrow$ large and

2. $\alpha = 0$ and $\beta \rightarrow$ large

When $\beta = 0$, Eq. 6 becomes:

$$f(w) = - {}_1F_1[a; 1; 2w^{1/2}] + a {}_1F_1[a+1; 2; 2w^{1/2}] \quad (21)$$

and it will be impossible to make $f(w) = 0$ if $w \leq \alpha$ (the second term is always larger than the first in Eq. 21), therefore, the first root, w_1 , of $f(w)$ must be greater than α .

The extreme condition in case 2 is when β goes into infinity. The following relationship is required to keep $f(w)$ finite:

$${}_1F_1[a; 1; 2w^{1/2}] = 0 \quad (22)$$

with $w_1 = 1.8284$. Eq. 22 is independent of β , which implies that the wall reaction will gradually decrease its contribution and eventually result in no effect on the concentration change of the reacting species as β grows. The diffusion process will then be the rate controlling step, instead. The initial guess for w_1 is therefore as follows:

$$w_1 = 1.8284 \text{ when } \alpha \text{ is small and } \beta \text{ is large, and}$$

$$w_1 = \alpha \text{ when } \alpha \text{ is large.}$$

The r th root of $f(w)$, if α is large, e.g., $\alpha \geq 100$, can be approximated by solving Eq. 14 for w , i.e.,

$$w_r - (2r - 1)w_r^{1/2} - \alpha = 0 \quad (23)$$

The accuracy of w_r from Eq. 23 improves as α gets larger and sustains regardless of how large β is, because the wall reaction can not compete with the fast bulk reaction and has a limited influence on concentration change of the species. Table 1 shows w_r is a very weak function of β . The remainder, $Re(w_r)$, obtained by substitution of w_r from Eq. 23 into Eq. 9, is

$$Re(w_1) = \beta - w_1^{1/2} \quad (24-1)$$

and

$$Re(w_r) = \left(\beta - w_r^{1/2} \right) \left(\sum_{i=0}^{r-1} \frac{(a)_i x^i}{(b)_i i!} \right) + 2w_r^{1/2} \left(\sum_{i=0}^{r-2} \frac{(a+1)_i x^i}{(b)_i i!} \right),$$

for $r \geq 2$ (24-2)

$Re(w_r)$ is negligible as compared with the values of $f(w)$, except those close to $f(w) = 0$.

Element 3: $f(w)$ is not a periodic function and a good method to modify the initial guess for the next eigenvalue is now necessary. Fig. 1 shows that any two consecutive eigenvalues, say w_i and w_{i+1} , have slopes of opposite sign. The following relationships are defined:

$$R_i = \left\{ (w) : \frac{df}{dw} \frac{df}{dw_i} \geq 0 \right\} \quad (25-1)$$

$$R_{i+1} = \left\{ (w) : \frac{df}{dw} \frac{df}{dw_i} < 0 \right\} \quad (25-2)$$

for every $w \leftarrow S_{i+1}$, where S_{i+1} is the possible domain of the initial guess for w_{i+1} . If the initial guess falls in

Table 1-1: Comparison between w_{true} and w_{estimate} at $\beta = 0$

$\lambda = 25.0$			$\lambda = 100.0$		
n	w_{true}	w_{estimate}	n	w_{true}	w_{estimate}
1	30.5225	30.5249	1	110.5125	110.5125
2	45.1090	45.1605	2	134.8356	134.8356
3	65.1415	65.4509	3	164.0384	164.0388
4	91.2421	92.2229	4	198.6602	198.6637
5	123.9064	126.0413	5	239.1756	239.1927
6	163.5941	167.2634	6	285.9800	286.0391

Table 1-2: Comparison between w_{true} and w_{estimate} at $\lambda = 100$

n	Estimated values		True values	
	$\beta = 0.0$	$\beta = 0.0$	$\beta = 100$	$\beta = 10000$
1	110.5125	110.5125	110.5125	110.5125
2	134.8356	134.8356	134.8356	134.8356
3	164.0388	164.0384	164.0391	164.0392
4	198.6637	198.6602	198.6661	198.6666
5	239.1927	239.1756	239.2044	239.2069
6	286.0391	285.9800	286.0794	286.0833

the region R_i , multiply it by some factor larger than unity. This procedure is repeated until the value goes into the region R_{i+1} , where the Newton-Raphson method applies.

Element 4: If the initial guess is near the peak or the bottom of the wave, the correction value may go into the unbounded region and a restriction on the maximum correction value, say 15% of the initial guess, is required. The first six eigenvalues are determined sufficient for the experimental conditions we have studied. The values of w_n and B_n are tabulated in Table 2, with α and β as parameters.

Table 2: Eigenvalues and function coefficients.

$\alpha = 0.00, \beta = 0.00$			$\alpha = 0.25, \beta = 0.25$		
n	w_n	B_n	n	w_n	B_n
1	0.0000	1.0000	1	0.8466	1.1694
2	6.4199	0.0000	2	7.5655	-0.2364
3	20.9655	0.0000	3	22.1510	0.1044
4	43.5416	0.0000	4	44.8016	-0.0619
5	74.1341	0.0000	5	75.4550	0.0423
6	112.7368	0.0000	6	114.1106	-0.0313

$\alpha = 0.50, \beta = 0.00$			$\alpha = 0, \beta = 0.5$		
n	w_n	B_n	n	w_n	B_n
1	0.9605	1.1180	1	0.6734	1.2013
2	7.4289	-0.1532	2	7.5030	-0.2929
3	21.9706	0.0513	3	22.2594	0.1467
4	44.5451	-0.0252	4	44.9922	-0.0931
5	75.1365	0.0150	5	75.7125	0.0663
6	113.7386	-0.0099	6	114.4249	-0.0506

$\alpha = 0.10, \beta = 0.1$			$\alpha = 0.5, \beta = 0.5$		
n	w_n	B_n	n	w_n	B_n
1	0.3726	1.0767	1	1.4865	1.2782
2	6.8674	-0.1051	2	8.4724	-0.4000
3	21.4497	0.0438	3	23.2484	0.1920
4	44.0543	-0.0256	4	45.9868	-0.1170
5	74.6702	0.0173	5	76.7092	0.0810
6	113.2931	-0.0127	6	115.4228	-0.0604

Table 2: (Continue)

$\alpha = 1.00$ $\beta = 1.00$			$\alpha = 2.50$ $\beta = 2.50$		
n	w_n	B_n	n	w_n	B_n
1	2.4726	1.3998	1	4.6815	1.5336
2	10.0850	-0.6014	2	13.5313	-0.8538
3	25.1820	0.3248	3	29.5235	0.5362
4	48.1313	-0.2079	4	53.1476	-0.3741
5	79.0146	0.1475	5	84.5718	0.2803
6	117.8606	-0.1119	6	123.8707	-0.2208

$\alpha = 25.0$ $\beta = 0.00$			$\alpha = 25.0$ $\beta = 100$		
n	w_n	B_n	n	w_n	B_n
1	30.5225	1.8048	1	30.5267	1.8010
2	45.1090	-1.4415	2	45.1952	-1.4268
3	65.1415	1.1369	3	65.6435	1.1142
4	91.2421	-0.8901	4	92.7921	-0.8766
5	123.9064	0.8915	5	127.2228	0.7051
6	163.5941	-0.5347	6	169.2519	-0.5823

$\alpha = 100$ $\beta = 0.00$			$\alpha = 0.0$ $\beta = 10,000$		
n	w_n	B_n	n	w_n	B_n
1	110.5125	1.9003	1	1.8283	1.4764
2	134.8356	-1.7034	2	11.1518	-0.8061
3	164.0384	1.5155	3	28.4789	0.5887
4	198.6602	-1.3411	4	53.8079	-0.4758
5	239.1756	1.1829	5	87.1376	0.4050
6	285.9800	-1.0351	6	128.4679	-0.3561

C. NUMERICAL SOLUTION

There is, however, a disadvantage in use of the analytical solution method, i.e., it takes significant computer time to calculate the eigenvalues. This becomes awkward when combined with the optimization (see below) where estimations of the eigenvalues are repeated many times. The equation of continuity is, therefore, solved using numerical techniques which are more efficient. The equation is transformed into a set of simultaneous finite difference equations using the Crank-Nicholson method.

The reactor is partitioned into 20 segments in the radial direction and 100 sections in the axial direction. We then have a set of 21 simultaneous finite difference equations which needs to be solved 100 times. The set of equations is:

$$E C'_{i-1,j+1} + F C'_{i,j+1} + G C'_{i+1,j+1} = A C'_{i-1,j} + B C'_{i,j} + C C'_{i+1,j} \quad (26-1)$$

where

$$E = \left(\frac{1}{4uh} - \frac{1}{2h^2} \right), \quad F = \left(\frac{1}{h^2} + \frac{4(1-u^2)}{k} + 2\alpha \right), \quad G = \left(\frac{-1}{4uh} - \frac{1}{2h^2} \right)$$

$$A = \left(\frac{1}{2h^2} - \frac{1}{4uh} \right), \quad B = \left(\frac{4(1-u^2)}{k} - \frac{1}{h^2} - 2\alpha \right), \quad C = \left(\frac{1}{2h^2} + \frac{1}{4uh} \right)$$

for interior points $2 \leq i \leq 20$,

$$\left(\frac{1}{h^2} + \frac{2}{k} + \alpha \right) C'_{1,j+1} - \frac{1}{h^2} C'_{2,j+1} = \left(\frac{2}{k} - \frac{1}{h^2} - \alpha \right) C'_{1,j} + \frac{1}{h^2} C'_{2,j} \quad (26-2)$$

for points on the center axis where L'Hospital's rule is used to treat the indeterminate case of $\frac{1}{u} \frac{\partial C'}{\partial u}$ as $u = 0$ and

where the boundary condition $C' = \text{finite}$ at $u = 0$ is applied to eliminate $C'_{0,j+1}$ and $C'_{0,j}$. And the relationship

$$\frac{-1}{h^2} C'_{20,j+1} + \left(\frac{1}{h^2} + \frac{2\beta}{h} + \beta + 2\alpha \right) C'_{21,j+1} = 0 \quad (26-3)$$

is utilized for points at the reactor wall where the

boundary condition $-\frac{\partial C'}{\partial u} = 2\beta C'$ at $u = 1$ is applied to

eliminate $C'_{22,j+1}$. The subscripts i and j refer to increments in the radial and axial directions respectively, with h and k respectively the corresponding spacing.

Eq. 26 is then solved by Gaussian elimination. A comparison of the analytical and numerical solutions in Table 3* shows excellent agreement. The numerical method, once α and β are given, needs less than one second cpu time on the UNIVAC 90/80-4 computer to get the reactant concentration profile at the reactor outlet, while it takes more than two second cpu time to do the same job by the analytical solution.

* Under our reaction conditions, computer simulation shows that the species concentration at some distance, z , of a reactor can be approximated at the outlet of the reactor by operating the reactor with a fluid velocity L/z times the original velocity.

Table 3: Comparison of analytical and numerical solutions with experimental results.

A: Reactor conditions

Radius: 0.2 cm	Length: 45.0 cm	
Temp.: 828 °K	Average velocity: 142	cm/sec
D: 2.03 cm ² /sec	k _b : 0.561 l/sec	k _w : 0.0038 cm/sec
Alpha: 0.00276	Beta: 0.000187	v*: 0.715

Note: $v^* = v/z$

B: Eigenvalues and function coefficients

n	Eigenvalue	Coefficient
1	0.0058	1.0008
2	6.4259	-0.0010
3	20.9716	0.0003
4	43.5478	-0.0002
5	74.1402	0.0001
6	112.7430	-0.0001

C: Cup-mixing-concentration

Distance(%)	Experimental	Analytical	Numerical
25	0.95	0.9537	0.9555
32	0.94	0.9411	0.9434
45	0.92	0.9182	0.9213
61	0.89	0.8907	0.8948
77	0.86	0.8641	0.8691
100	0.82	0.8272	0.8335

D: SSR between experimental & analytical calculations:

0.0000873

Table 3: (Continue)

A: Reactor conditions

Radius: 0.5 cm	Length: 45.0 cm	
Temp. : 828 °K	Average velocity: 71.0 cm/sec	
D: 2.03 cm ² /sec	k _b : 0.561 l/sec	k _w : 0.0038 cm/sec
Alpha: 0.0173	Beta: 0.000468	v*: 0.229 l/cm

Note: $v^* = v/z$

B: Eigenvalues and function coefficients

n	Eigenvalue	Coefficient
1	0.0354	1.0046
2	6.4556	-0.0059
3	21.0014	0.0019
4	43.5777	-0.0010
5	74.1701	0.0006
6	112.7728	-0.0004

C: Cup-mixing-concentration

Distance(%)	Experimental	Analytical	Numerical
33	0.89	0.8866	0.8877
38	0.88	0.8706	0.8718
44	0.85	0.8518	0.8531
52	0.82	0.8273	0.8288
63	0.79	0.7948	0.7966
77	0.75	0.7552	0.7573
100	0.70	0.6945	0.6970

D: SSR between experimental and analytical calculations:

0.000237

Table 3: (Continue)

A: Reactor conditions

Radius: 0.4 cm	Length: 45.0 cm
Temp. : 828 °K	Average velocity: 81.0 cm/sec
D: 2.03 cm ² /sec	k_b : 0.561 1/sec k_w : 0.0038 cm/sec
Alpha: 0.0111	Beta: 0.000374 v^* : 0.313 1/cm

Note: $v^* = v/z$

B: Eigenvalues and function coefficients

n	Eigenvalue	Coefficient
1	0.0228	1.0030
2	6.4430	-0.0038
3	20.9887	0.0013
4	43.5649	-0.0006
5	74.1575	0.0004
6	112.7502	-0.0002

C: Cup-mixing-concentration

Distance(%)	Experimental	Analytical	Numerical
24	0.93	0.9257	0.9265
28	0.91	0.9138	0.9148
38	0.89	0.8849	0.8861
46	0.87	0.8624	0.8638
56	0.85	0.8351	0.8367
73	0.79	0.7906	0.7929
100	0.73	0.7248	0.7274

D: SSR between experimental and analytical calculations:

0.000366

Table 3: (Continue)

A: Reactor conditions

Radius: 0.2 cm	Length: 45.0 cm	
Temp. 881 °K	Average velocity: 102 cm/sec	
D: 2.26 cm ² /sec	k_b : 2.66 1/sec	k_w : 0.0570 cm/sec
Alpha: 0.0118	Beta: 0.00252	v^* : 1.11 1/cm

Note: $v^* = v / z$

C: Eigenvalues and function coefficients

n	Eigenvalue	Coefficient
1	0.0285	1.0044
2	6.4499	-0.0058
3	20.9964	0.0021
4	43.5732	-0.0011
5	74.1662	0.0007
6	112.7695	-0.0005

C. Cup-mixing-concentration

Distance (%)	Experimental	Analytical	Numerical
19	0.75	0.7633	0.7657
22	0.71	0.7314	0.7339
35	0.60	0.6080	0.6108
60	0.44	0.4261	0.4287
78	0.35	0.3299	0.3322
100	0.24	0.2413	0.2433

D: SSR between experimental and analytical calculation:

0.00130

Table 3: (Continue)

A: Reactor conditions

Radius: 0.5 cm	Length: 45.0 cm	
Temp.: 881 °K	Average velocity: 45.4 cm/sec	
D: 2.26 cm ² /sec	k _b : 2.66 1/sec	k _w : 0.0570 cm/sec
Alpha: 0.0736	Beta: 0.00631	v*: 0.398 1/cm

Note: $v^* = v/z$

B: Eigenvalues and function coefficients

n	Eigenvalue	Coefficient
1	0.1583	1.0218
2	6.5833	-0.0284
3	21.1310	0.0097
4	43.7090	-0.0050
5	74.3027	0.0031
6	112.9066	-0.0021

C: Cup-mixing-concentration

Distance(%)	Experimental	Analytical	Numerical
19	0.61	0.5832	0.5847
31	0.43	0.4149	0.4162
36	0.31	0.3601	0.3612
57	0.18	0.1984	0.1992
80	0.14	0.1033	0.1038
100	0.10	0.0586	0.0589

D: SSR Between experimental and analytical calculations:

0.00690

Table 3: (Continue)

A: Reactor conditions

Radius: 0.4 cm	Length: 45.0 cm	
Temp.: 906 °K	Average velocity: 90.7 cm/sec	
D: 2.38 cm ² /sec	k _b : 9.15 l/sec	k _w : 0.280 cm/sec
Alpha: 0.154	Beta: 0.0235	v*: 0.328 l/cm

Note: $v^* = v/z$

B: Eigenvalues and function coefficients

n	Eigenvalue	Coefficient
1	0.3463	1.0506
2	6.7880	-0.0665
3	21.3415	0.0238
4	43.9242	-0.0126
5	74.5218	0.0080
6	113.1292	-0.0056

C: Cup-mixing-concentration

Distance(%)	Experimental	Analytical	Numerical
25	0.28	0.2784	0.2796
28	0.24	0.2388	0.2398
47	0.081	0.0904	0.0908
76	0.026	0.0205	0.0206
89	0.008	0.0106	0.0106
100	0.006	0.0060	0.0060

D: SSR between experimental and analytical calculations:

0.000130

Table 3: (Continue)

A: Reactor conditions

Radius: 0.2 cm	Length: 45.0 cm	
Temp.: 906 °K	Average velocity: 190 cm/sec	
D: 2.38 cm ² /sec	k _b : 9.15 1/sec	k _w : 0.280 cm/sec
Alpha: 0.0384	Beta: 0.0118	v*: 0.626 1/cm

Note: $v^* = v/z$

B: Eigenvalues and function coefficients

n	Eigenvalue	Coefficient
1	0.0995	1.0163
2	6.5268	-0.0216
3	21.0765	0.0080
4	43.6559	-0.0044
5	74.2511	0.0029
6	112.8562	-0.0020

C: Cup-mixing-concentration

Distance(%)	Experimental	Analytical	Numerical
31	0.43	0.4193	0.4216
40	0.35	0.3258	0.3277
56	0.21	0.2080	0.2094
65	0.15	0.1616	0.1628
75	0.11	0.1221	0.1230
82	0.080	0.1003	0.1011
100	0.061	0.0606	0.0611

D: SSR between experimental and analytical calculations:

0.00140

Table 3: (Continue)

A: Reactor conditions

Radius: 0.1 cm	Length: 45.0 cm	
Temp.: 954 °K	Average velocity: 1100 cm/sec	
D: 2.60 cm ² /sec	k _p : 9.97 l/sec	k _w : 4.47 cm/sec
Alpha: 0.00959	Beta: 0.0860	v*: 0.472 l/cm

Note: $v^* = v/z$

B: Eigenvalues and function coefficients

n	Eigenvalue	Coefficient
1	0.1776	1.0491
2	6.6528	-0.0684
3	21.2297	0.0302
4	43.8301	-0.0182
5	74.4428	0.0127
6	113.0631	-0.0095

C: Cup-mixing-concentration

Distance(%)	Experimental	Analytical	Numerical
34	0.29	0.2765	0.2813
42	0.21	0.2043	0.2080
55	0.12	0.1250	0.1273
72	0.069	0.0658	0.0670
92	0.021	0.0309	0.0315
100	0.033	0.0229	0.0233

D: SSR between experimental and analytical calculations:

0.000450

Table 3: (Continued)

A: Reactor conditions

Radius: 0.2 cm	Length: 45.0 cm	
Temp.: 954 °K	Average velocity: 506 cm/sec	
D: 2.60 cm ² /sec	k _b : 9.97 l/sec	k _w : 4.47 cm/sec
Alpha: 0.0383	Beta: 0.172	v*: 0.257 l/cm

Note: $v^* = v/z$

B: Eigenvalues and function coefficients

n	Eigenvalue	Coefficient
1	0.3669	1.0961
2	6.9122	-0.1346
3	21.5227	0.0605
4	44.1487	-0.0367
5	74.7822	0.0255
6	113.4208	-0.0191

C: Cup-mixing-concentration

Distance(%)	Experimental	Analytical	Numerical
44	0.17	0.1541	0.1569
52	0.11	0.1097	0.1118
63	0.057	0.0688	0.0701
77	0.027	0.0380	0.0387
89	0.019	0.0228	0.0233
100	0.016	0.0143	0.0146

D: SSR between experimental and analytical calculations:

0.000531

D. OPTIMIZATION

To determine the values of k_b and k_w of the reacting species from experimental data, the sum of the squares of the residuals (SSR), now needs to be minimized.

$$\text{Minimize } SSR(k_b, k_w) = \sum_{i=1}^N (C_{\text{calc},i} - C_{\text{expt},i})^2 \quad (27)$$

The C_{calc} and C_{expt} are the cup-mixing-concentrations, calculated and experimental respectively, and N is the number of experimental data points.

The technique to obtain the optimum (positive) values of k_b and k_w makes use of the Response Surface Method (RSM) (Box and Wilson, 1951; Box, Hunter, and Hunter, 1978) which was originally designed as a sequential approach to attain optimum operating conditions with a minimum number of experiments. In this RSM, the response is the SSR, and the factors are k_b and k_w . The RSM now becomes an optimization algorithm capable of estimating k_b and k_w .

Fig. 2 shows some typical results of the simulation. It is no surprise that there exist an infinite number of pairs of optimum k_b and k_w (continuous curve), all of which permit the calculated concentrations to fit the experimental data for a specified reactor.

Fig. 3 shows the corresponding response surface

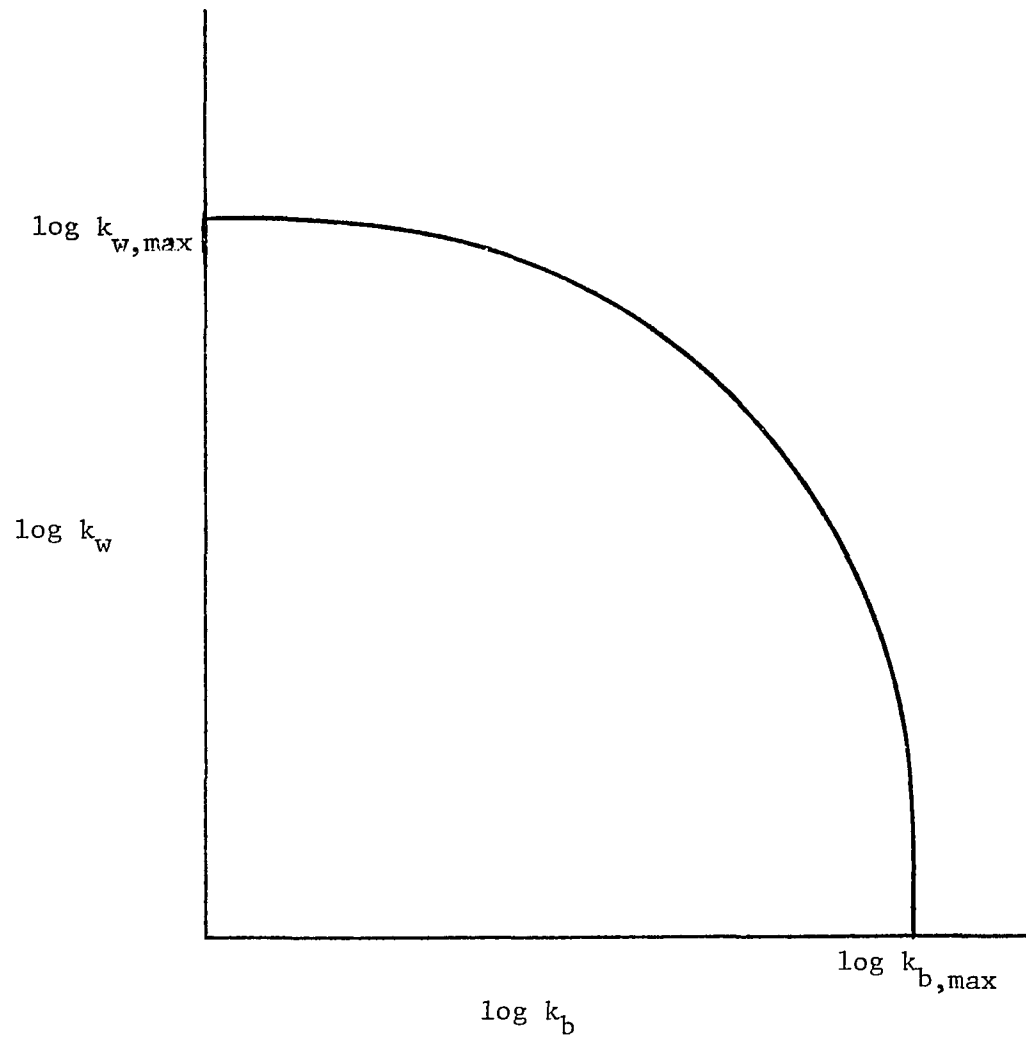


Fig 2: The continuous curve is constituted by an infinite number of pairs of the coupled optimum $\log k_b$ and $\log k_w$.

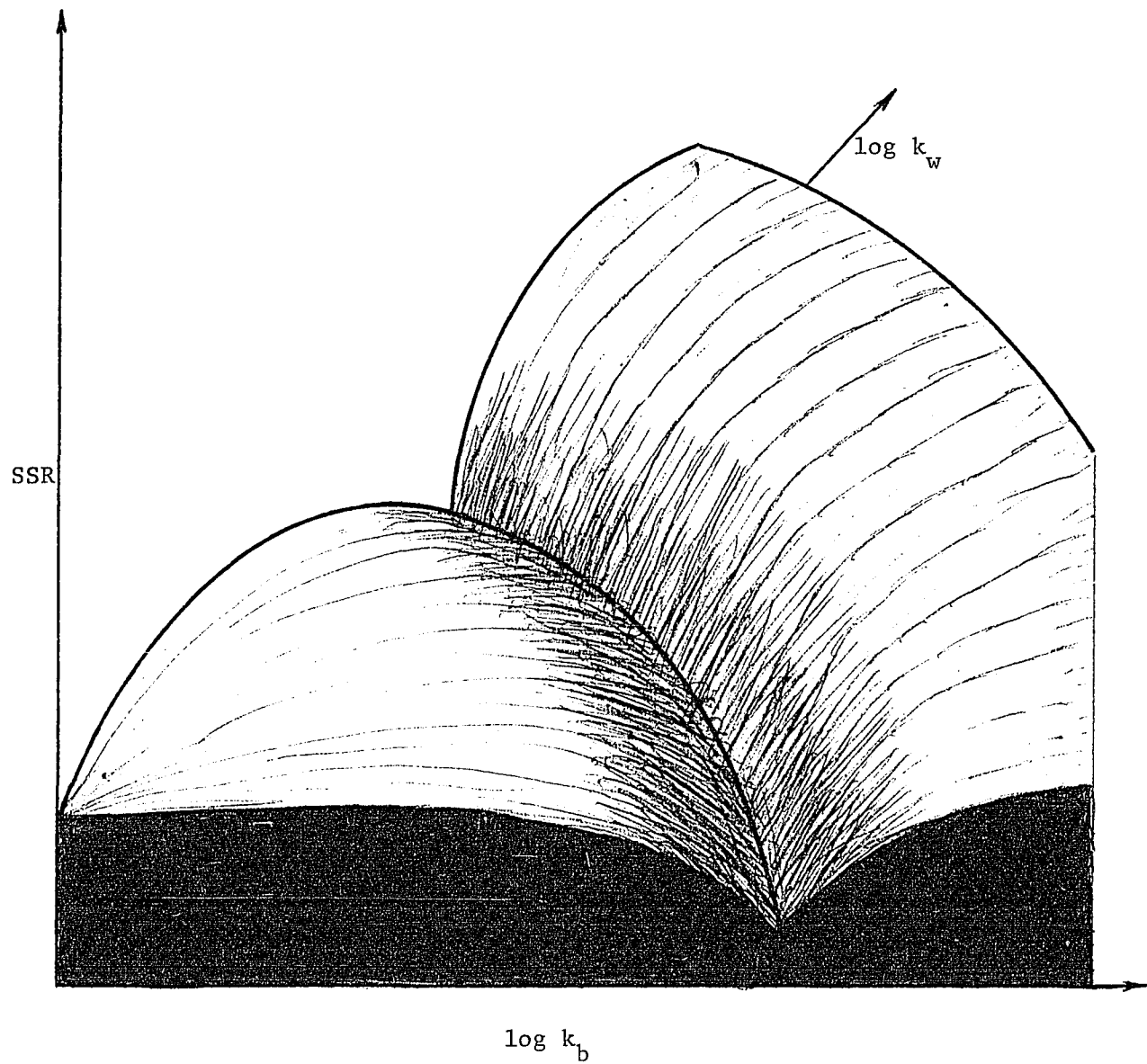


Fig. 3: Response Surface represents SSR versus $\log k_b$ and $\log k_w$.

representing the SSR versus $\log k_b$ and $\log k_w$. It contains a long, narrow valley, which is composed of the minimum SSR values. It is the monotony of the surface that allows the facile evaluation of optimum k_b and k_w , while it is the continuous valley that makes determination of the true k_b and k_w difficult.

It will be convenient to define the following relationships for further analysis in this calculational procedure:

$$k_{b,\max} = k_b + f(k_w, R) \quad (28-1)$$

$$k_{w,\max} = k_w + g(k_b, R) \quad (28-2)$$

where, $f(k_w, R)$ is the wall rate constant based on the unit bulk volume of a reactor, and $g(k_b, R)$ the bulk rate constant based on the unit wall area of the same reactor. Eq. 28-1 becomes Eq. 17 if the plug-flow model is valid.

E. DECOUPLING

If a substance undergoes two parallel reactions whose mechanisms are unknown and/or whose products indistinguishable, it may be difficult to determine the individual rate constants from the experimental data. Fig. 2 demonstrates that an infinite number of points on the k_b vs k_w curve satisfy the required optimization criterion and the optimization technique fails to locate the specific (true) values for k_b and k_w .

The system consisting of bulk and wall reactions is, however, a special case of two parallel reactions. The relative contribution of the wall reaction depends on the surface area of reactor, while the relative contribution of the homogeneous phase reaction is a function of the reactor volume. The ratio of the wall to the bulk reaction rate is, therefore, a function of the surface to volume ratio, $2/R$. The reactions are run with reactors of different $2/R$ ratio, and under other similar reaction conditions so that differences in reaction extent can be observed. The optimum k_b vs k_w curve shown in Fig. 2 will be different for the different S/V ratios. The results of this simulation is shown in Fig. 4, demonstrating that different curves are indeed obtained and that the curves intersect, yielding single, true, k_b and k_w values.

The larger diameter reactor, with smaller S/V ratio,

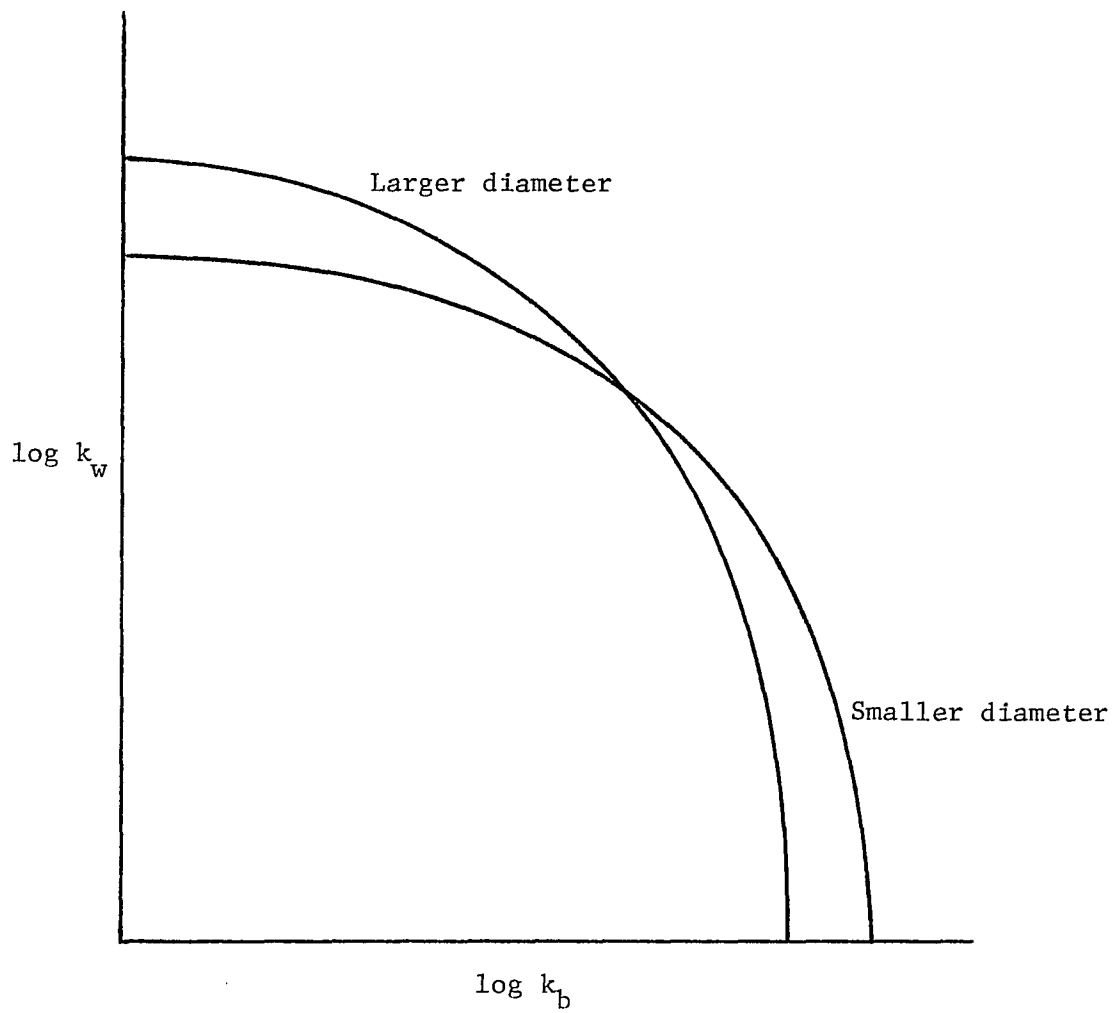


Fig. 4: The intersection of two curves characterized by diameter gives the true values of $\log k_b$ and $\log k_w$.

has a smaller $f(k_w, R)$ value. Thus its $k_{b,max}$ value is lower than that of the smaller (larger S/V) reactor. On the other hand, its $k_{w,max}$ value is larger than that of the smaller reactor (see Eq. 28). The true values of k_b and k_w are at the intersection, and as shown in Fig. 4; they are acceptable to both reactors and are independent of diameter. They are the actual kinetic rate constants.

F. LIMITING CONDITIONS

The relationship demonstrated by Kaufman(1961)

$$k_{\text{expt}} = k_b + \frac{2}{R}k_w \quad (17)$$

is, additionally, valid for plug-flow reactor conditions. It states that k_{expt} depends upon the radius of the reactor. In general, k_{expt} is the sum of k_b and $f(k_w, R)$ as shown in Eq. 28. Fig. 4 shows that k_{expt} approaches k_b as R gets larger, and that k_b becomes negligible as R gets smaller. k_b , therefore, may be approximated by k_{expt} when a large reactor is employed, while k_w may be approximated by $(R/2)k_{\text{expt}}$ when a small reactor is employed. The latter is explained by observing that both α and β become smaller as the radius gets smaller. Under such a condition, the plug-flow approximation is valid and Eq. 17 is applicable. It is obvious that the magnitude of the reactor employed to determine either rate constant depends on the ratio of k_b to k_w .

G. VALIDITY OF PLUG-FLOW MODEL

A laminar-flow system with boundary conditions as stated above may, if its (α, β) is less than (0.25, 0.50), be represented by the plug-flow model considering radial-dispersion. It can moreover be approximated by the plug-flow model, if the dimensionless length, v , is sufficiently small.

The parabolic radial concentration profile of a reacting species begins to develop once the fluid flows into the reactor, causing a deviation from the plug-flow pattern. The difference between the concentrations calculated by the laminar- and the plug-flow models will grow with a decreasing acceleration as the fluid flows down the reactor, even though the deviation of the true radial concentration profile from the uniform profile may remain small. There is therefore a "curvature" in the vicinity of the origin as $\ln(C_{\text{calc}})$ vs v is plotted (Poirier and Carr, 1971).

The validity of the plug-flow model therefore depends on v as well as α and β . Simulation shows that the plug-flow model will underestimate the concentration of the reacting species in a system with (α, β) being equal to (0.01, 0.01) by more than 5% at $v = 200$, and a -10% error is expected at $v = 0.5$ for a system with (0.25, 0.50).

H. BULK REACTION VERSUS WALL REACTION

The concentration change of a reacting species in a tubular-flow reactor is modeled by Eq. 1. The bulk reaction occurs everywhere in the reactor, while the heterogenous reaction is confined at the wall of the reactor. This difference distinguishes the influence of α and β on the concentration change. We may take α as a system property and β , a boundary property.

Boundary condition 3 states that the amount of reagent consumed by the wall reaction comes from the radial dispersion. The wall reaction would cease if there were no diffusion to the wall. The bulk reaction can, on the other hand, sustain itself by depleting "local" molecules of the species. Dispersion in the radial direction can supply sufficient amount of the reacting species to the wall only when the wall reaction rate, more accurately, β , is small. β is therefore competitive with α when α is small, and Eq. 19 is valid. The effect of β on the axial concentration change, however, weakens and, eventually, dies as β increases.

One interesting phenomenon is that $f(0) = \beta$ (Eq. 10) but w_1 approaches 1.8284 (Eq. 22) when $\alpha = 0$. The species concentration on the wall is high enough to sustain the wall reaction at the reactor entrance and $f(0) = \beta$. A radial concentration gradient is immediately created, as the fluid

moving down the reactor, to slow down the rate of the species disappearance, which is then solely determined by the radial dispersion and w_1 approaches 1.8284 no matter how large β is.

A wall reactor (with fast wall reaction and negligible bulk reaction), e.g., is characterized by β and v (Sec. II.G). Its performance can be improved by optimizing the value of β , that means we should keep a balancing $k_w/(2D/R)$ ratio while trying to increase the k_w values. The concentration change would solely be controlled by v , which, in turn, is a function of D/R^2 (Smith, Krieger, and Herzog, 1980) as well as z/V_0 if β is too large. The best way to improve the performance of a wall reactor is to operate the reactor in the fully developed turbulent condition so that the rapid eddy transport can bring sufficient molecules to the laminar sublayer close to the reactor wall (Bird, Stewart, and Lightfoot, 1960).

III. EXPERIMENTAL

A. APPARATUS

A diagram of the experimental apparatus (Mahmood, 1985) is shown in Fig. 5. The tubular flow reactor was made of quartz, which was maintained at a constant temperature (within ± 3 °C, over more than 80 % of the 45 cm-length reactor) by a three-zone oven. A higher quantity of energy per unit length, or volume, of the reactor was input by the end heaters in order to partially nullify the higher heat losses experienced there.

A heating tape type preheater was also mounted on the reactor, which had 15 cm of length and brought the reactor inlet temperature up to 400 °C (no reaction observed at the preheat zone).

The reagents and products exited the reactor and flowed through a glass wool filtering media to contain the carbon particulate, and to destroy the laminar-flow pattern. The on-line gas chromatograph (parallel electron capture and flame ionization detectors) analyzed the sample quantitatively, and a GC/Mass Spectrometer was routinely used to qualitatively verify the GC peak identifications.

The halocarbon reagent used (1,1,1-trichloroethane) was added to a hydrogen reagent stream using two saturaters

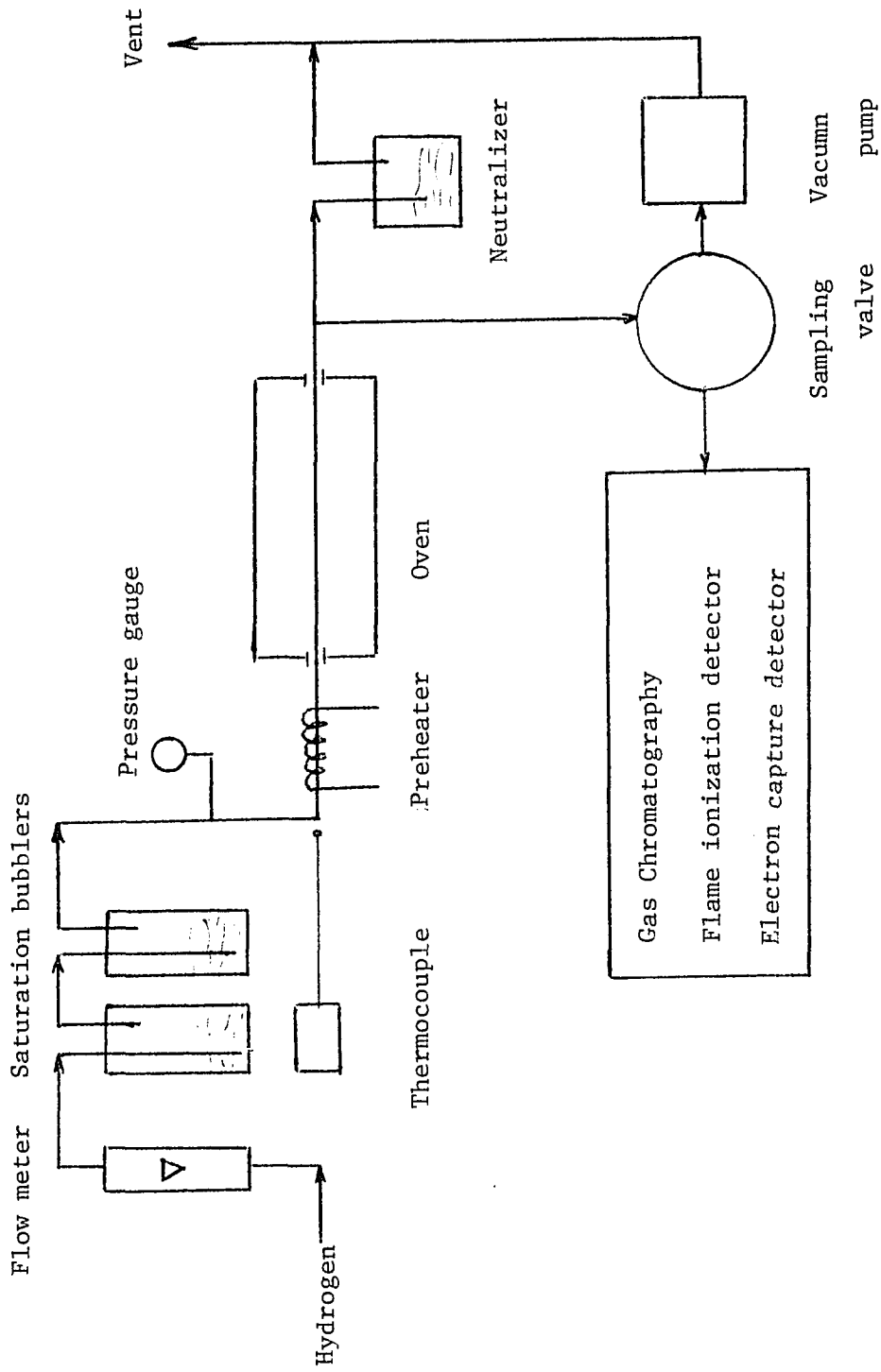


Fig. 5: Experimental apparatus.

(evaporators) in series, at 5 °C. The 99% 1,1,1-trichloroethane was supplied by the Aldrich Chemical Co.. The 99.99% hydrogen and the 99.99% nitrogen (used in GC) were purchased from the MG Scientific Gases.

In this study, two different reactor diameters are required, as a minimum to determine the specific rate constants, k_p and k_w . The diameters of reactors ranged from 0.2 to 1.0 cm and they were 45 cm long in length. The gas velocities ranged from 45 to 1200 cm/sec, and depended on hydrogen flow rate and reactor diameter. The operating pressure was 1.05 atm. Four temperatures were run, 828, 881, 906 and 954 °K, where kinetic data over a significant range of conversion were obtainable.

The initial concentration of 1,1,1-trichloroethane was calculated by the ideal gas law assuming that the hydrogen gas became saturated with the halocarbon at the liquid bath temperature. The molar ratio of 1,1,1-trichloroethane to hydrogen in this study was 1:16, and the molecular diffusion coefficient was estimated using the formula correlated by Fuller, Schettler and Giddings (FSG) (1960). The more accurate Chapman-Enskog formula was not used to estimate the diffusion coefficient, because the required parameters were not obtainable for 1,1,1-trichloroethane. The FSG method is accurate in this study because of high operating temperatures (Marrero and Mason, 1973) combined with the low

critical temperature of hydrogen (Nain and Ferron, 1972),
for this binary system.

B. EXPERIMENTAL RESULTS

The experimental data on decomposition of 1,1,1-trichloroethane, as shown in Fig. 6 and 7, exhibits good linearity for first-order rate equations, demonstrating that the first-order assumptions used in Eq. 1 is valid.

It is also clear that the extent of decomposition of 1,1,1-trichloroethane depends on reactor diameter and that the difference between conversions in reactors of different diameter becomes larger as temperature increases.

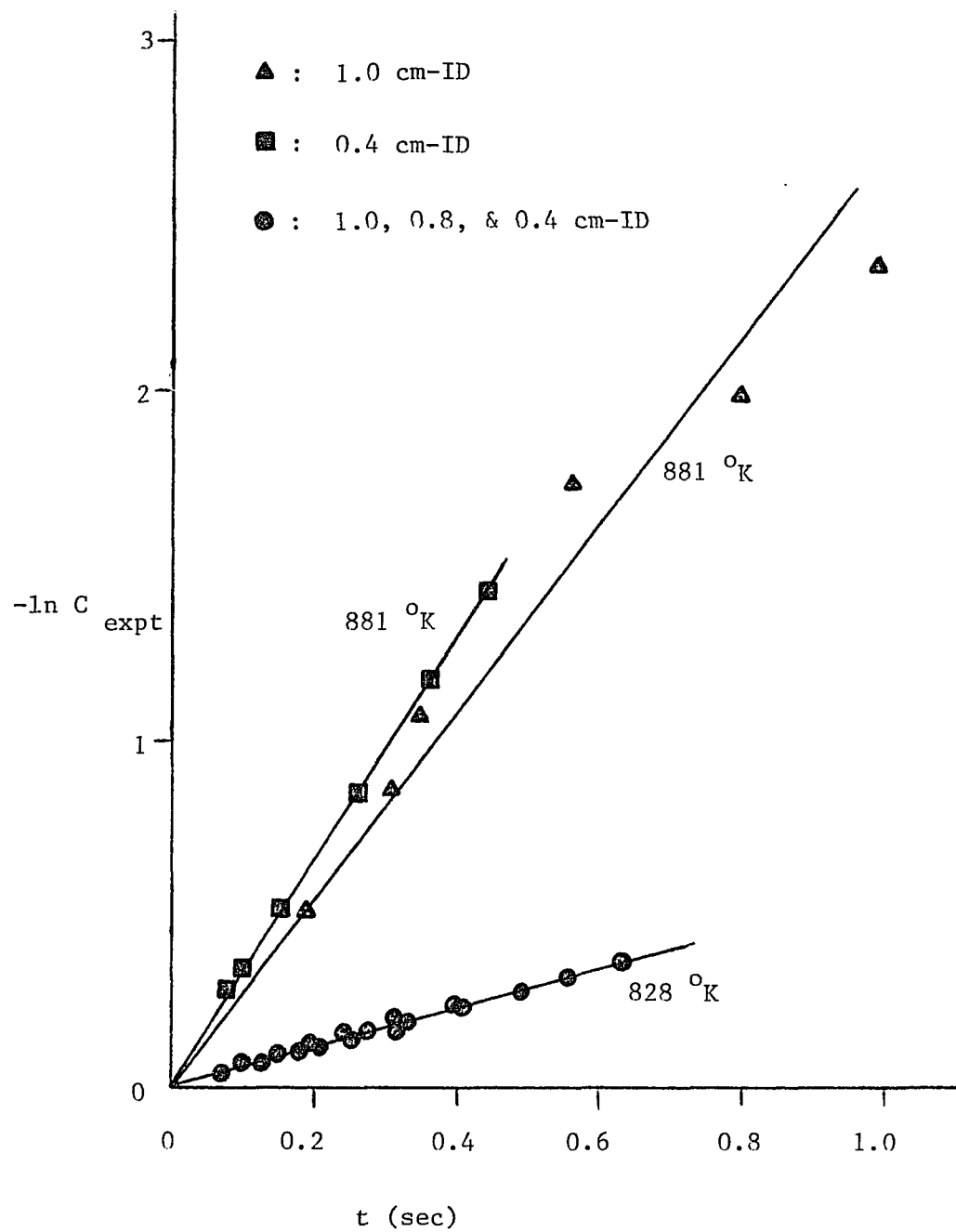


Fig. 6: Concentration-time curves for the pyrolysis of 1,1,1-trichloroethane in the presence of hydrogen.

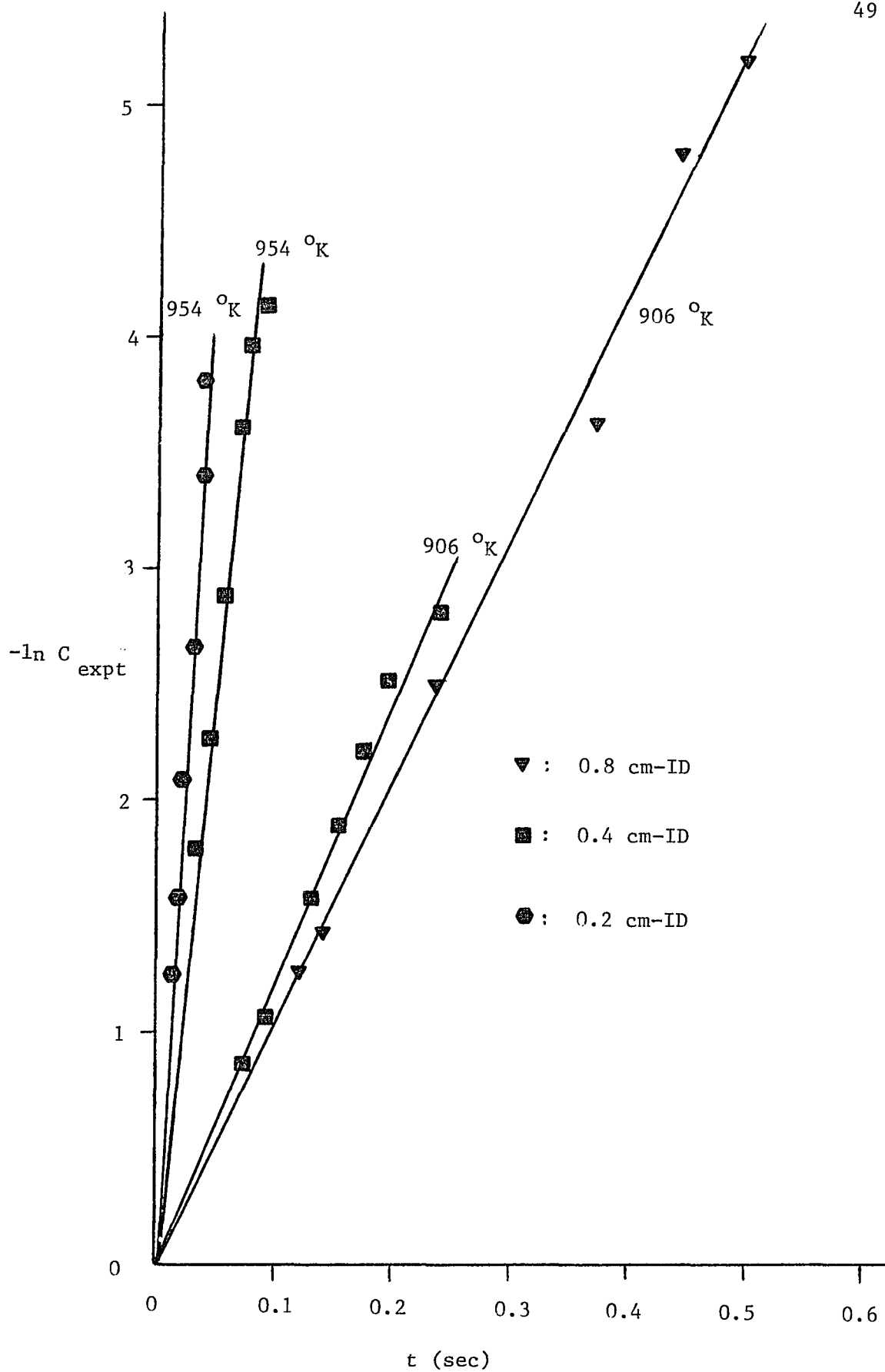


Fig. 7: Concentration-time curves for the pyrolysis of 1,1,1-trichloroethane in the presence of hydrogen.

C. KINETIC MODELLING OF LAMINAR-FLOW REACTOR

Fig. 8 shows the results of optimization and decoupling. Each pair of the true k_b and k_w lies on the corresponding intersection of the optimum curves. Fig. 9 shows the same results as those of Fig. 8 at 828 °K, only with largely expanded coordinates, illustrating the clear curve crossing which is difficult to observe in Fig. 8. The intersections formed by these three curves do not coincide because of experimental error, and the centroid of the intersections gives the true values of k_b and k_w .

Table 4 and Fig. 10 show the dependencies of k_b and k_w on temperature. The wall reaction of 1,1,1-trichloroethane exhibits more than twice the activation energy of the bulk reaction. The corrected values of activation energies still have a significant difference (Sec. III.F). This may be explained by

1. A radical recombination mechanism effectively reversing the initial decomposition steps proposed for wall reaction.
2. A more likely "stabilization" of the activated 1,1,1-trichloroethane species by the surface, reducing the initial decomposition rate and/or limiting secondary reactions.
3. A combination of (1) and (2) above.

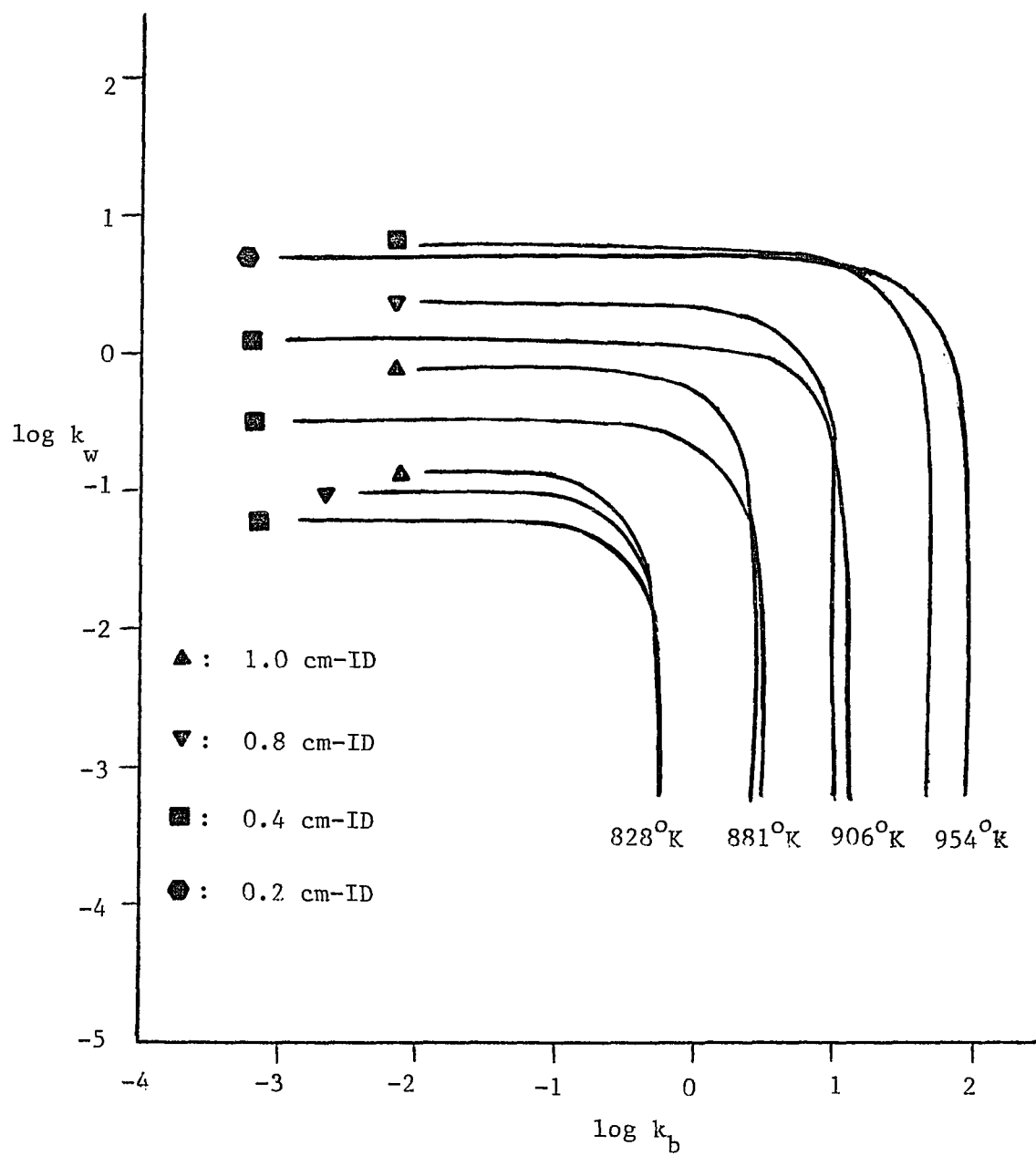


Fig. 8: The intersection of curves in each set gives the true $\log k_b$ and $\log k_w$ for the pyrolysis of CH_3CCl_3 in H_2 .

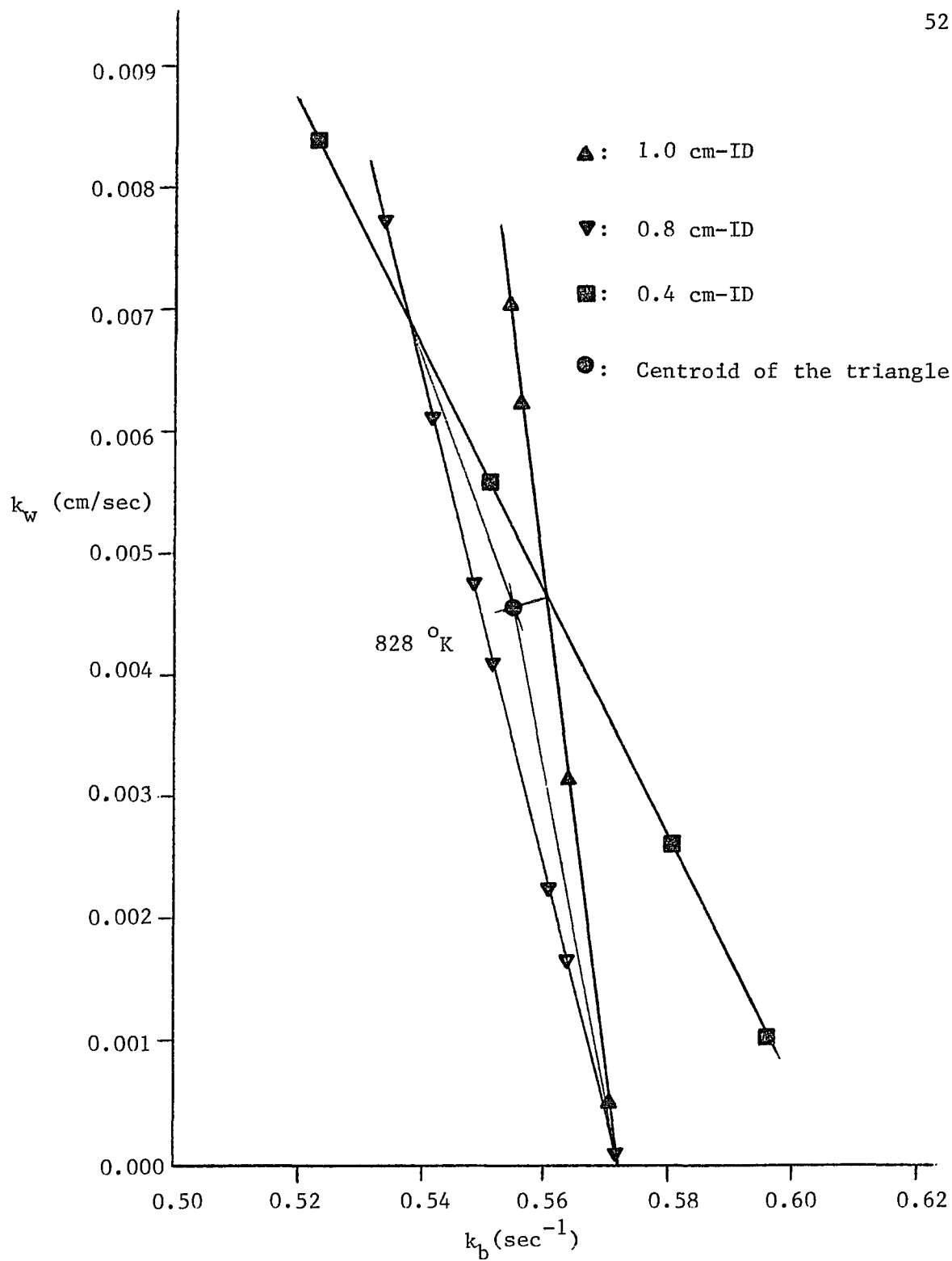


Fig. 9: The center of gravity of the triangle gives the true values of k_b and k_w .

Table 4: k_b and k_w with temperature.

T (°K)	k_b (1/sec)	k_w (cm/sec)
828	0.561	0.0038
881	2.66	0.0570
906	9.15	0.281
954	9.97(30.1)	4.47 (1.86)
E/R (°K)	20,500 (25,300)	44,300 (37,900)
A (1/sec)	3.36×10^{10} (1.09×10^{13})	4.83×10^{20} (3.51×10^{17})

Note: Number in the bracket is the corrected value.

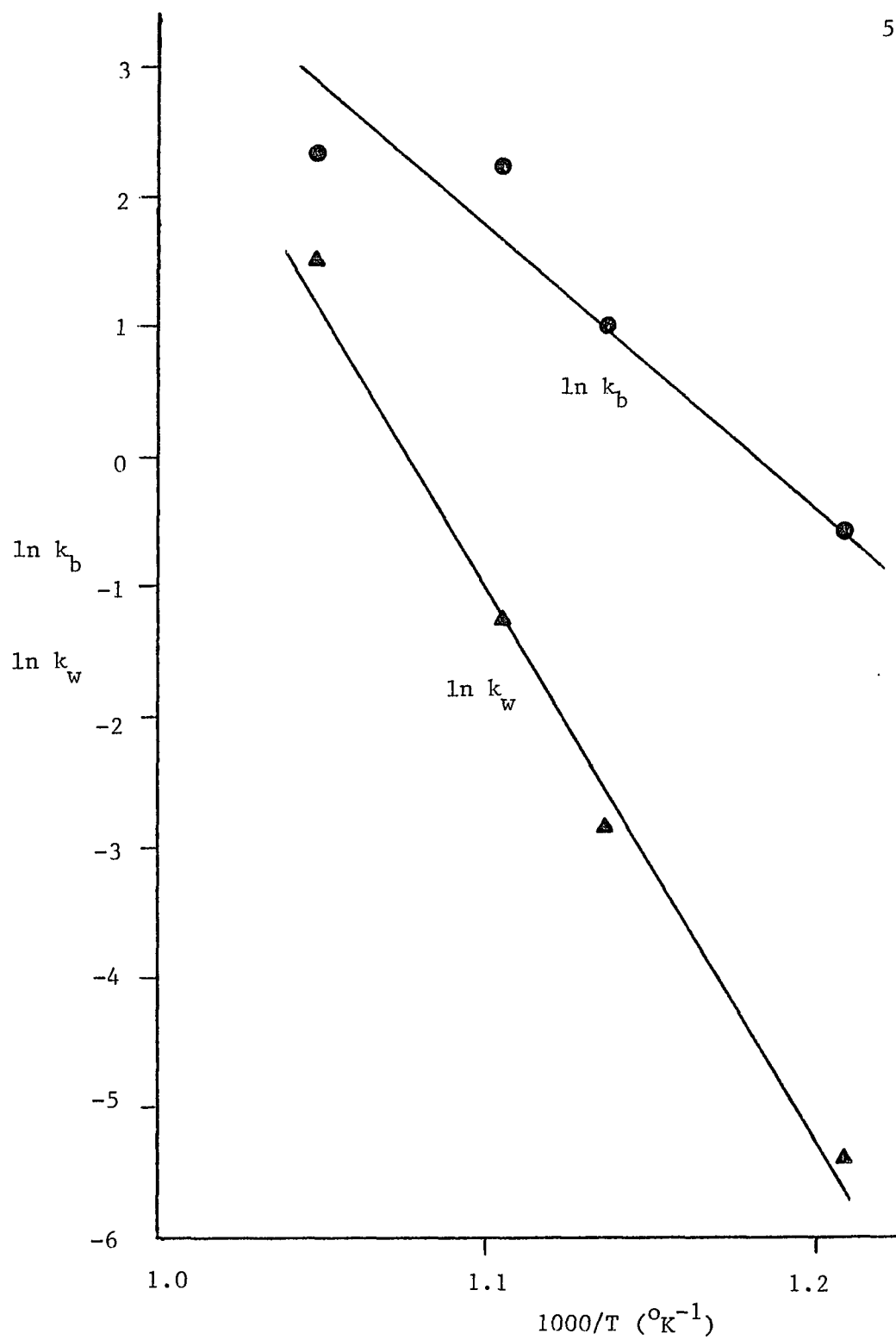


Fig. 10: Dependencies of rate constants on temperature.

D. COMPARISON OF ANALYTICAL- WITH NUMERICAL- SOLUTIONS

The cup-mixing-concentrations along reactor length were calculated once the true k_D and k_W values were obtained, and were compared with experimental data, as shown in Table 3. The results show that the analytical- and the numerical solutions are in excellent agreement and that both fit the experimental data (The SSR is a measure of deviation of the analytical- from the experimental- concentrations). It is clear, because of small values of α and β , that the point concentration is weakly dependent on the radial distance, and that the first term in the analytical solution dominates, which is observed from the fast decay of function coefficients.

E. COMPARISON WITH PLUG-FLOW MODEL

The reacting systems [except those at 954 °K because of the high (α , β , v) values, Sec.II.G] can be well represented by the plug-flow model. The k_{expt} values, based upon the plug-flow model, are also calculated and are shown in Table 5. A plot of k_{expt} versus $2/R$ is shown in Fig. 11 for the experimental data at four temperatures: 954, 906, 881 and 828 °K. The slopes yield the wall rate constants, k_w , and the intercepts give the bulk rate constant, k_b , as described in Eq. 17. Table 6 presents the results of the wall and the bulk rate constants in addition to those obtained from the numerical solution of the continuity equation with the optimization procedure described. The results are in remarkably good agreement considering the extremely different calculational paths. This agreement clearly illustrates the value of the plug-flow model for the reactor conditions used in this study.

Table 5: k_{expt} (1/sec) as calculated using the plug-flow model

Radius(cm)		0.1	0.2	0.4	0.5
Temp. (°K)	828	---	0.605	0.572	0.571
	881	---	3.23	---	2.59
	906	---	12.1	10.4	---
	954	87.5 (67.3)	48.8	---	---

Note: Number in the bracket is the corrected value.

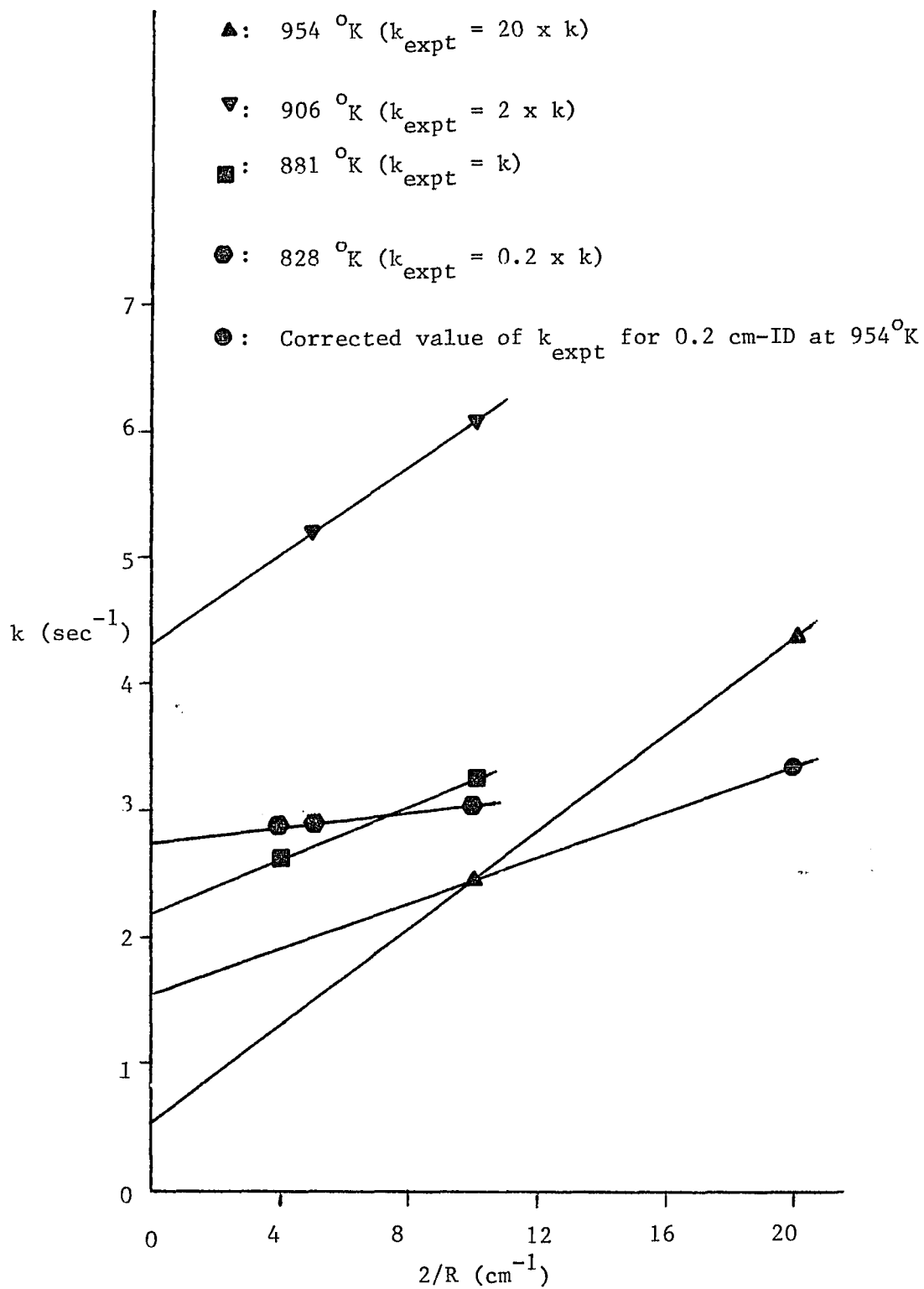


Fig. 11: k_b and k_w from the plug-flow model.

Table 6: Comparison of k_b and k_w ---
 laminar- versus plug- flow models

T(°K)	k_b (1/sec)		k_w (cm/sec)	
	Laminar	Plug	Laminar	Plug
828	0.561	0.537	0.0038	0.0057
881	2.66	2.17	0.0570	0.107
906	9.15	8.70	0.281	0.340
954	9.97(30.1)	11.2(30.7)	4.47(1.86)	3.87(1.85)

Note: Number in the bracket is the corrected value.

F. CORRECTION OF RATE CONSTANTS

The necessity for correction resulted from the use of the 0.2 cm-ID reactor. The decomposition reaction was so vigorous at 954 °K that a 0.2 cm-ID reactor operating at higher space-velocity was needed to obtain significant data for the kinetic analysis. It was impossible to directly measure the temperature profile in this reactor because of the size of the thermocouple being comparable with the diameter of reactor. The 0.2 cm-ID reactor was instead assumed to have the same temperature as that in the 0.4 cm-ID reactor. The correction on k_b and k_w was possible by observing that there should be a straight line formed when the intersections of curves in Fig. 8 are connected because both $\ln k_b$ and $\ln k_w$ are inversely proportional to temperature. Fig. 12 shows that the intersection of this straight line with the 0.4 cm-ID's curve gives the corrected k_b and k_w values which are 30.1 l/sec and 1.86 cm/sec, respectively, as shown in Table 4. The corrected dependencies of k_b and k_w on temperature are in Fig. 13. The corrected activations and frequency factors are also included in Table 4. The rate equations we obtained are

$$k_b = 1.09 \times 10^{13} \text{Exp}(-25,300/T) \quad (29)$$

$$k_w = 3.51 \times 10^{20} \text{Exp}(-37,900/T) \quad (30)$$

The corrected value of k_{expt} in the 2 cm-ID reactor at 954 °K is 67.3 sec⁻¹, as shown in Table 5. The corrected k_b

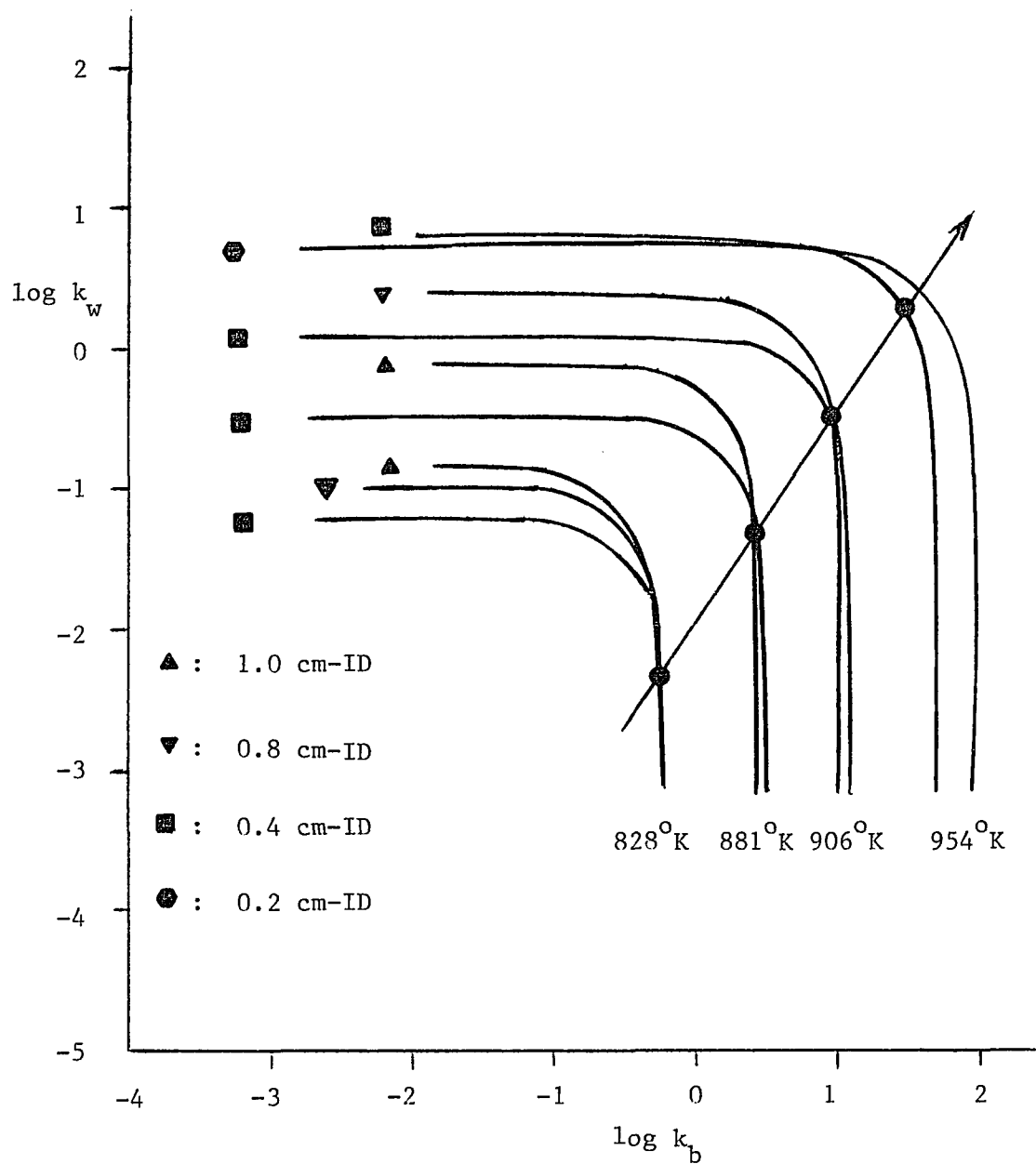


Fig. 12: k_b and k_w at 954°K are corrected by extrapolating the straight $\log k_w - \log k_b$ line to the 0.4 cm-curve at 954°K .

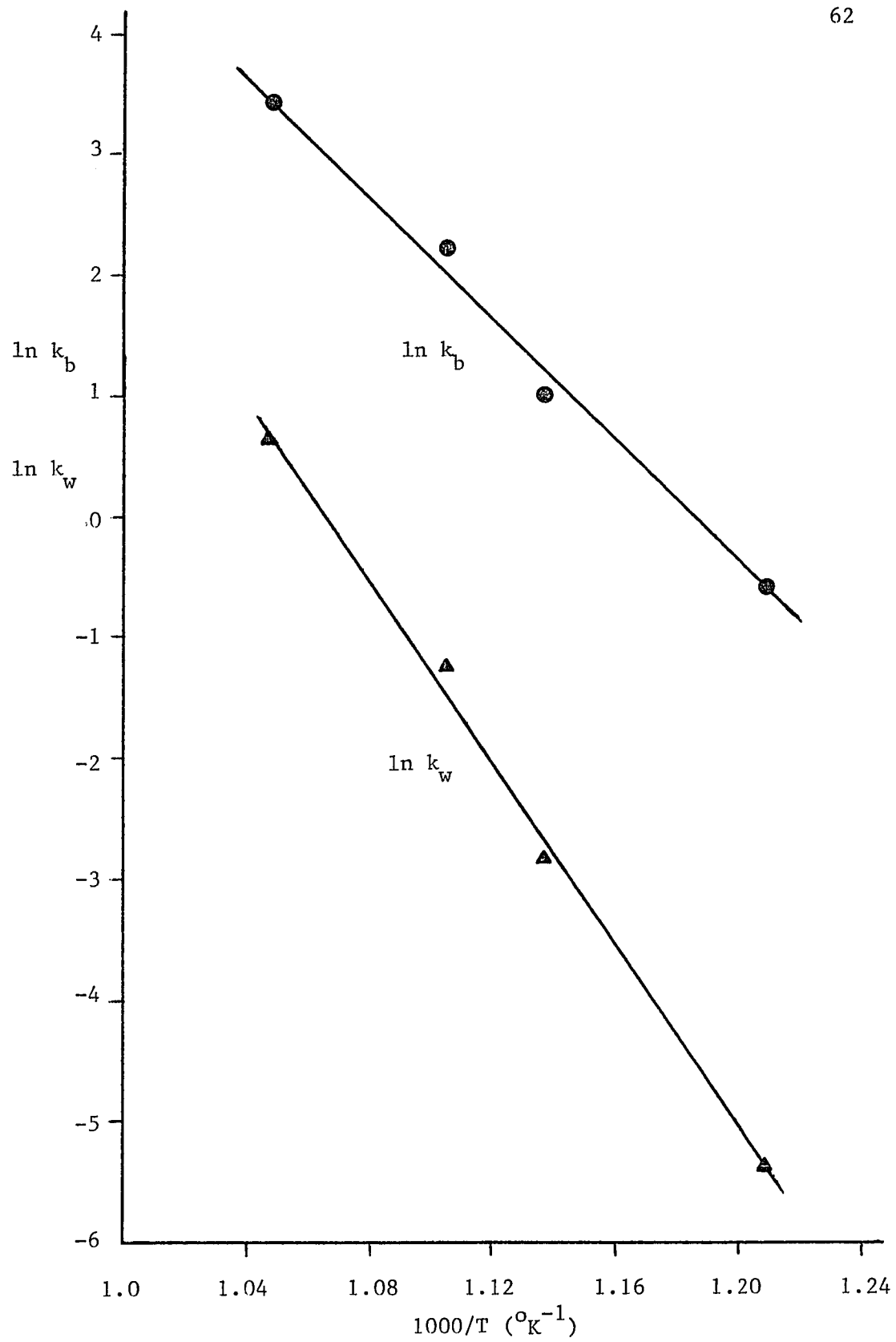


Fig. 13: The values of k_b and k_w at 954°K are corrected.

and k_w are accordingly 30.7 sec^{-1} and 1.85 cm/sec , respectively (Fig. 11 and Table 6).

G. COMPARISON OF RATE CONSTANTS WITH LITERATURE VALUES

It is worthy of comparing the rate constants of the 1,1,1-trichloroethane decomposition with literature values, though the decomposition conditions are not the same. It should be noted that 1,1,1-trichloroethane was, in the previous studies, not diluted with hydrogen gas.

Barton and Onyon (1950) studied 1,1,1-trichloroethane thermal decomposition in static reactors in the temperature range 635.7 to 707.0 °K. Their results showed that the wall inhibited the decomposition reaction because the proposed "key" free radical, $\cdot\text{CH}_2\text{CCl}_3$ was consumed faster at the wall. They reported that the first-order rate constant for homogeneous unimolecular decomposition can be represented by $10^{14}\text{Exp}(-54,000/\text{RT}) \text{ sec}^{-1}$.

Benson and Spokes (1967), using the very low pressure technique, covered a high temperature range (890 to 1265 °K). The corresponding high pressure rate equation is $10^{13.8}\text{Exp}(-51,700/\text{RT}) \text{ sec}^{-1}$.

The decomposition of 1,1,1-trichloroethane in this research study occurred in a hydrogen mixture at 1 atm total pressure. Each radical formed in this environment had an opportunity to react with hydrogen, causing the mechanism somewhat different from that proposed by Barton and Onyon. The combination of the two radicals, $\cdot\text{CH}_2\text{CCl}_3$ and $\text{Cl}\cdot$, in

Barton and Onyon's model might, e.g., not occur or have a very low rate if hydrogen were abundant.

Fig. 14 illustrates an interesting comparison of the data. The high activation energy associated with wall reaction makes its rate constant negligible at low temperatures but the wall reaction does increase steeply with temperature. The reaction extent is therefore effectively due to the bulk reaction at low temperatures, while the wall reaction can dominate at high temperatures. The wall and the bulk rate constant equations serve as asymptotes to the previous experimental rate constant equation at, respectively, high temperatures and low temperatures.

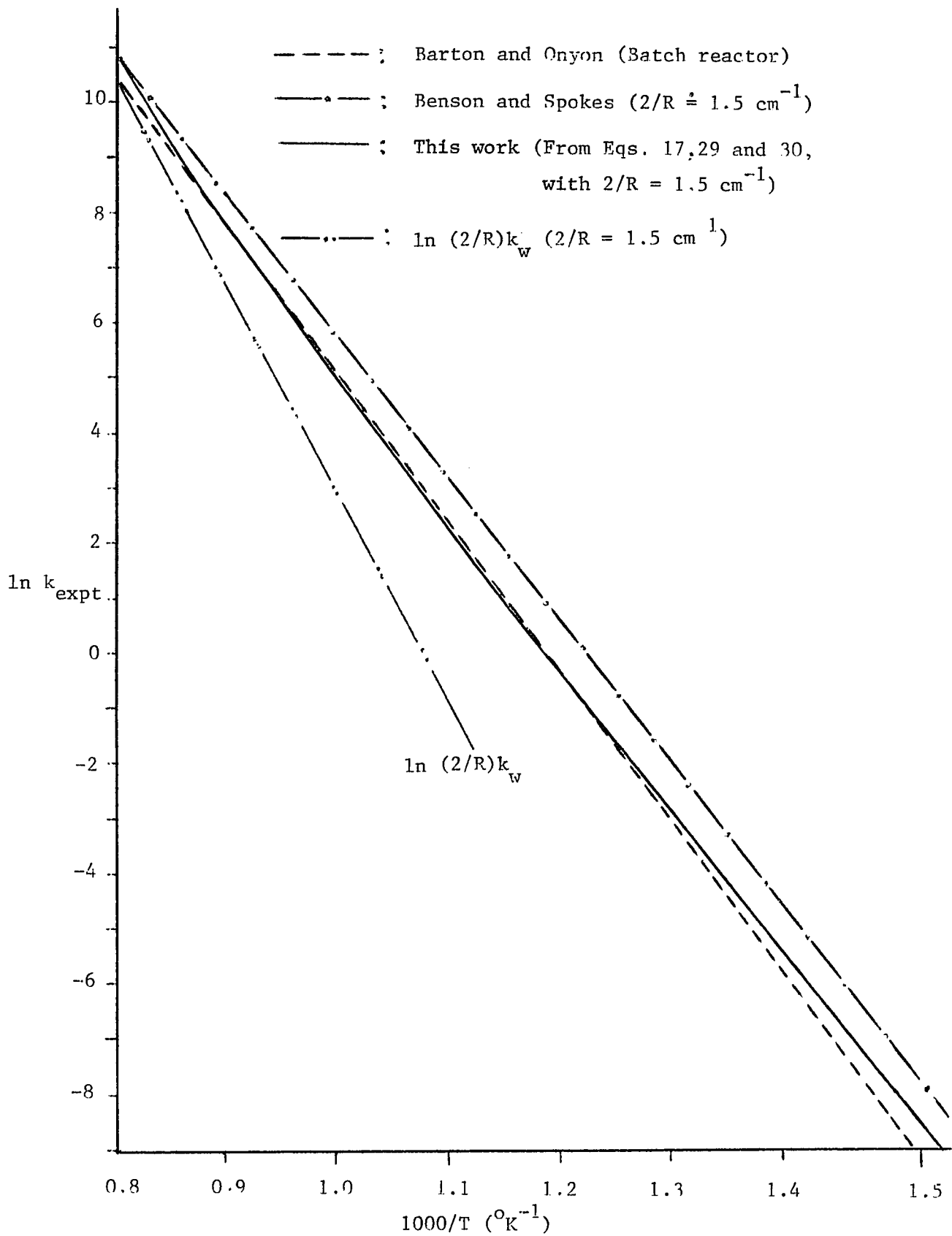


Fig. 14: Comparison with literature values.

H. ERROR ANALYSIS

The experimental rate constant, k_{expt} , is

$$k_{\text{expt}} = F_T \frac{T}{273} \frac{760}{P} \frac{1}{\pi R^2} \frac{d(\ln C_{\text{expt}})}{dz} \quad (31)$$

The cumulative value of the relative error of k_{expt} (Howard, 1979; Cvetanović, Singleton and Paraskevopoulos, 1979), can be written as

$$\frac{\Delta k_{\text{expt}}}{k_{\text{expt}}} = \left[\left(\frac{\Delta F_T}{F_T} \right)^2 + \left(\frac{\Delta T}{T} \right)^2 + \left(\frac{\Delta P}{P} \right)^2 + \left(2 \frac{\Delta R}{R} \right)^2 + \left(\frac{\Delta \text{Slop}}{\text{Slop}} \right)^2 \right]^{1/2} \quad (32)$$

Table 7 summarizes the estimated precision of individual measurements. The principal error is measurement of fluid, which consists of errors in measurement of hydrogen flow rate and evaporation of 1,1,1-trichloroethane into hydrogen.

The operating temperature employed for this kinetic study ranged from 828 to 954 °K, much higher than 600 °K, the upper limit specified by Howard. It is difficult to maintain a uniform axial temperature profile when the reactor is operating at a high temperature like that over 800 °K. There existed nonisothermal regions at each end of the reactor, from which, though, we had tried to nullify the higher heat losses. Mahmood (1985) performed correction on the nonisothermal data (Froment and Bischoff, 1979), and his results showed that an approximate (positive) 5% correction is required on each of k_b and k_w from the reactors when the

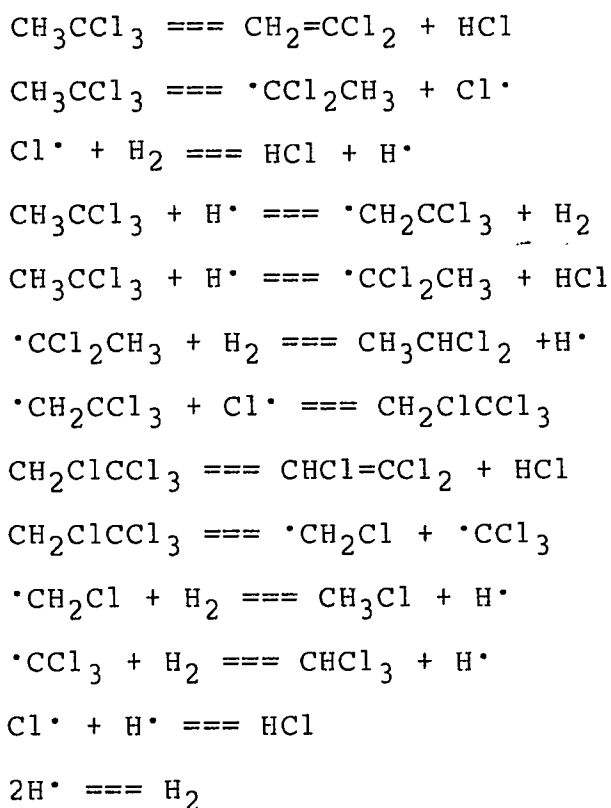
Table 7: Estimated Precision with 95% Confidence Interval

Measurement X	$\Delta X/X$		Note
	Normal	This study	
F_T	0.03	0.06	
T	0.01	0.01	+3 °K
P	0.01	0.01	
R	0.01	0.02	Deposit of carbon particles
Slope	0.02	0.02	
k_{expt}		0.13	
k_b and k_w		0.13	From Eq. 17

reference temperature is based on the most probable temperature in the reactor.

I. MECHANISM

The major products from the reaction were observed to be 1,1-dichloroethylene (vinylidene chloride), chloroform, 1,1-dichloroethane, trichloroethylene, methylene chloride, 1,1,1,2-tetrachloroethane and hydrogen chloride. The initiation step suggested by Barton and Onyon (1950) was supported by the above products and adopted here. The possible mechanism is as follows



Mathematical modeling on the mechanism of the decomposition of trichloroethane needs further study (See Appendix 6).

IV. CONCLUSIONS

A. CONTINUITY EQUATION

The laminar-flow model, Eq. 1 (Sec. II.A), representing the concentration change of a reacting species in a tubular-flow reactor, was analytically solved by the separation of variables, as well as numerically by the Crank-Nicolson finite-difference method (Sec. II.C). The analytic solution, Eq. 5, contains the confluent hypergeometric function.

Solution of a partial differential equation by separation of variables results in a problem of solving for eigenvalues and their corresponding eigenfunctions. The determination of these eigenvalues is usually a major fraction of the work. The present study yielded an efficient method to obtain the first several eigenvalues of interest. It also provided, based on the stiffness of $f(w)$ when \mathcal{L} is large (100, e.g.), an accurate approximate to the eigenvalues.

Three important dimensionless variables, \mathcal{L} , β and v were defined. The validity of the plug-flow model depends on them. The values of \mathcal{L} and β are, when both of them are less than 0.01, exchangeable so that Eq. 17 is applicable at v up to 200. The effect of β on the reagent concentration change decays when β increases, which can be observed from

the convergence of the first eigenvalue to 1.8284 if there is no bulk reaction (Sec. II.B). Generally speaking, the concentration change in a wall reactor will be controlled by radial dispersion if β is larger than 5 (Smith, Krieger, and Herzog, 1980). The concentration change will always be affected by α , as seen from the fact that the first eigenvalue always increases with increasing α .

The validity of the plug-flow model depends also on v , because the difference in concentrations calculated at some v by the laminar-flow and plug-flow models will affect the difference at the next v . There would, for example, be an underestimate of 10% at $v = 0.5$ by the plug-flow model to a laminar-flow system with (α, β) being equal to (0.25, 0.50) (Sec. II.G).

B. RATE CONSTANTS

It is the purpose of this paper to obtain the bulk and the wall rate constants from the experimental data. We have, in order to fulfill this purpose: (1) set up the model and solved it (Sec. II.A to II.C); (2) obtained optimum values of k_b and k_w by the RSM (Sec. II.D); and finally, (3) located the true values of k_b and k_w by decoupling the interaction between them (Sec. II.E).

The computer simulation revealed that the response surface, representing the SSR versus $\log k_b$ and $\log k_w$, monotonically increases outwards from the long, narrow valley, which is composed of the minimum SSR values. The simulation also showed that the curve projected by the valley is a function of the reactor diameter. This parameter therefore serves as the decoupler to identify the true values of k_b and k_w .

The rate constants in a laminar-flow reactor can be calculated by the plug-flow model (Sec. II.G) if α , β and v are small. There exists a mutual limitation condition among α , β and v for the plug-flow model to be valid. A laminar-flow system with, e.g., $(\alpha, \beta, v) \leq (0.25, 0.50, 0.50)$ may be represented by the plug-flow model.

k_b or k_w can be determined alone if a large or small diameter reactor is chosen (Sec. II.F), respectively. The

required size of the reactor depends, however, on the relative magnitude of k_b to k_w because k_{expt} is a function of radius (Eq. 17 and Eq. 28)

C. THERMAL DECOMPOSITION OF 1,1,1-TRICHLOROETHANE

A majority of 1,1,1-trichloroethane decomposed into 1,1-dichloroethylene and hydrogen chloride at temperatures ranging from 828 to 954 °K, where both the wall reaction as well as the bulk reaction were significant. The overall rate of decomposition obeyed first-order kinetic equations (Figs. 6 and 7). The rate constants obtained from the laminar-flow model were

$$k_b = 1.09 \times 10^{13} \text{Exp}(-25,300/T) \text{ 1/sec } \pm 13\%, \text{ and}$$

$$k_w = 3.51 \times 10^{17} \text{Exp}(-37,900/T) \text{ cm/sec } \pm 13\%$$

For the system studied, α , β and v were within the plug-flow regime.

NOTATIONS

$$a = \frac{1}{2} - \frac{w - \alpha}{2w^{1/2}}$$

$$(a)_r = a(a+1)(a+2)\dots(a+r-2)(a+r-1).$$

$$(a)_t^M = a(a+1)(a+2)\dots(a+M-1)(a+M+1)\dots(a+t-2)(a+t-1).$$

B_n = Function coefficient.

$C = C(r, z)$ = Point concentration of species, moles/cm³.

C_0 = Concentration of species at reactor inlet, moles/cm³.

$$C' = C'(u, v) = \frac{C}{C_0} = \text{Normalized point concentration.}$$

$C_{\text{calc}}, C_{\text{expt}}$ = Normalized cup-mixing-concentrations.

D = Diffusion coefficient, cm²/sec.

F_T = Total gas flow rate, cm³/sec.

$${}_1F_1[a; b; x] = \sum_{r=0}^{\infty} \frac{(a)_r x^r}{(b)_r r!}.$$

$f(w)$ = eigenvalue equation.

$f(k_w, R)$ = k_w expressed in 1/sec.

$g(k_b, R)$ = k_b expressed in cm/sec.

k_b = Bulk rate constant, 1/sec.

k_{expt} = Experimental(apparent) rate constant, 1/sec.

k_w = Wall rate constant, cm/sec.

$k_{b, \text{max}}, k_{w, \text{max}}$: Defined in Eq. 26

L = Length of the reactor, cm

P = Reactor pressure, atm.

R = Radius of the reactor, cm.

r = Radial distance in the reactor, cm.

S = Surface of a reactor, cm^2 .

SSR = Sum of the squares of the residuals.

T = Reactor temperature, $^{\circ}\text{K}$.

$$u = \frac{r}{R}$$

V = Volume of a tubular reactor, cm^3 .

V_0 = Fluid velocity along the central line of the reactor, cm/sec.

$$v = \frac{4Dz}{V_0 R^2}$$

w_n = eigenvalue.

z = Axial distance in the reactor, cm.

$$\alpha = \frac{k_b R^2}{4D}$$

$$\beta = \frac{k_w R}{2D}$$

APPENDIX I. SOME PHYSICAL PROPERTIES OF HYDROGEN
AND 1,1,1-TRICHLOROETHANE*

	H ₂ (A)	CH ₃ CCl ₃ (B)
Molecular weight (M), grams/mole	2.0158	133.41
Melting point (mp), °C	-259.4	-30.4
Boiling point (bp), °C	-252.8	74.1
Lennard-Jones potential parameters		
σ , Å	2.827	---
ϵ/k , °K	59.7	---

* Reid, Prausnitz, and Sherwood, 1976.

APPENDIX 2. VAPOR PRESSURE OF 1,1,1-TRICHLOROETHANE

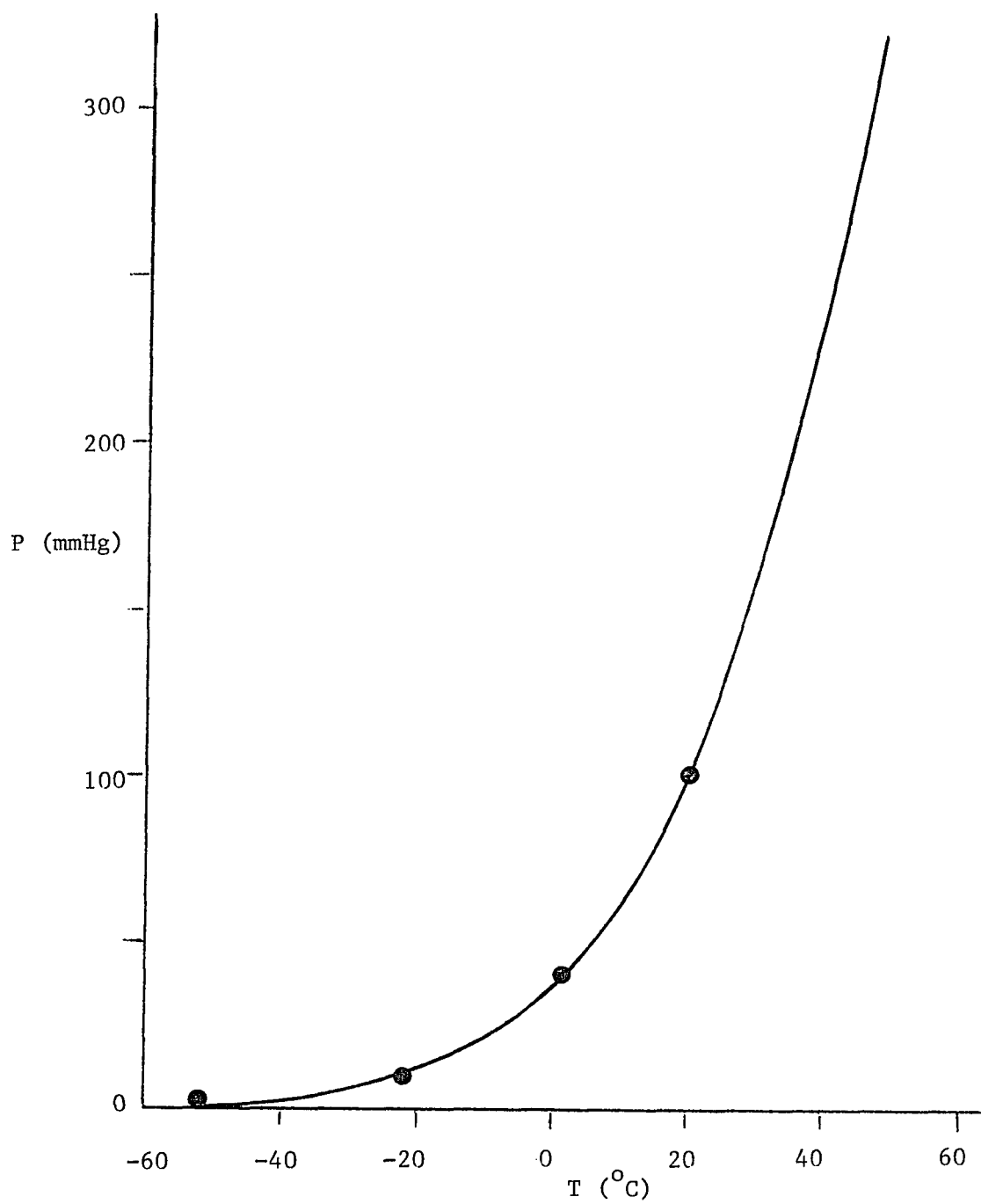


Fig. A1: Vapor pressure of 1,1,1-trichloroethane.

APENDIX 3. CALCULATION OF RENOLDS NUMBER

The laminar-flow pattern is valid if the Reynolds number of the fluid is below 2100. The mixture density was calculated by the ideal gas law; its viscosity was approximated by that of hydrogen, which in turn was calculated by the Chapman-Enskog formula (Reid, Prausnitz, and Sherwood, 1976). High limits of the N_{Re} were obtained because of low viscosity values of hydrogen.

Sample Calculation:

A fluid with an average velocity of 142 cm/sec flows in a 0.4 cm ID reactor at 828 °K and 1.05 atm. The composition of the fluid is 94.1% H₂(A) and 5.9% CH₃CCl₃(B).

The density of the mixture:

$$\begin{aligned} \rho &= \frac{MP}{RT} = \frac{(M_A X_A + M_B X_B)P}{RT} & (A1) \\ &= \frac{(2.02 \times 0.941 + 133. \times 0.059) \times 1.05}{82.05 \times 828} \\ &= 1.51 \times 10^{-4} \text{ (grams/cm}^3\text{)} \end{aligned}$$

The viscosity of hydrogen:

$$\begin{aligned} \mu &= 26.69 \times (MT) / (\sigma^2 \Omega_v) & (A2) \\ &= 26.69 \times (2.02 \times 828)^{1/2} / (2.827^2 \times 0.785) \\ &= 1.75 \times 10^{-4} \text{ grams/(sec-cm)} \end{aligned}$$

where

$$\Omega_v = \frac{A}{T^*B} + \frac{B}{\text{Exp}(DT^*)} + \frac{F}{\text{Exp}(ET^*)} \quad (\text{A3})$$

$$= \frac{1.16145}{13.90.14874}$$

$$= 0.785$$

where

$$T^* = \frac{k}{\epsilon} T \quad (\text{A4})$$

$$= \frac{1}{59.7} \times 828$$

$$= 13.9$$

Thus,

$$N_{Re} = \frac{RV_0 \rho}{\mu} \quad (\text{A5})$$

$$= \frac{0.4 \times 142 \times 1.51 \times 10^{-4}}{1.75 \times 10^{-4}}$$

$$= 49.0$$

Table A1: The ranges of N_{Re} at various diameters and temperatures

Dimeter (cm)	Temperature (°K)			
	828	881	906	954
0.2	---	---	---	151 - 444
0.4	49.0 - 199	52.3 - 268	57.0 - 186	139 - 318
0.8	56.2 - 235	---	54.4 - 220	---
1.0	61.6 - 187	58.2 - 305	---	---

APENDIX 4. CALCULATION OF DIFFUSION COEFFICIENT

The empirical correlation suggested by Fuller, Schettler and Giddings (1960) was used to calculate the diffusion coefficient of an A-B binary system. It is

$$D = \frac{0.001T^{1.75}[(M_A + M_B)/(M_A M_B)]^{0.5}}{P[(\sum v)_A^{1/3} + (\sum v)_B^{1/3}]^2} \quad (A6)$$

where T is kelvins and P, atmospheres. The value of the atomic diffusion volume for each atom of concern (Reid, Prausnitz, and Sherwood, 1976) is

$$C = 16.5 \quad H = 1.98 \quad Cl = 19.5 \quad H_2 = 7.07$$

Sample calculation:

Diffusion coefficient of H₂ (A) - CH₃CCl₃ (B) binary system at 828 °K and 1.05 atm.

$$(\sum v)_A = 7.07,$$

$$(\sum v)_B = 16.5 \times 2 + 1.98 \times 3 + 19.5 \times 3 = 97.4$$

Thus,

$$D = \frac{0.001 \times 828^{1.75}[(2.02 + 133.)/(2.02 \times 133.)]^{0.5}}{1.05(7.07^{1/3} + 97.4^{1/3})^2}$$

$$= 2.03(\text{cm}^2/\text{sec})$$

Table A2: Diffusion coefficients at various temperatures.

Temperature (°K)	Diffusionn Coefficient (cm ² /sec)
828	2.03
881	2.26
906	2.38
954	2.60

APENDIX 5. LISTING OF COMPUTER PROGRAMS

A. ANALYTICAL SOLUTION

A1. GENERAL GUIDES

This program calculates the cup-mixing-concentration of the reacting species modeled by Eq. 1 (Sec. II.A). The integration method to obtain the function coefficients and cup-mixing-concentrations is the Gauss-Legendre Quadrature (Fifteen-point formula). The program may need some modifications if λ is large (i.e., 5.0). These modifications include:

- (1) Increase the array containing the eigenvalues, W(9) [4 & 125], e.g., to W(15), and NW [9 & 126] to 15.
- (2) Reduce the values of the constants, 1.1 [155], 0.1 [164], and 1.40 [170].

The program will be out of work if $\lambda > 100$, because it doesn't include the special treatment as described in Eq. (15) (Sec. II.B).

Note: The number in [] stands for the statement number in the program.

A2. IDENTIFICATION VARIABLES IN DATA BLOCK

- ND: Number of experimental data.
- TR: Reactor diameter, cm.
- TZ: Reactor length, cm.
- TEM: Reactor temperature, °K.
- D: Binary diffusion coefficient, cm²/sec.
- VA: Minimum of average velocities, cm/sec.
- BK: Bulk rate constant, sec⁻¹.
- WK: Wall rate constant, cm/sec.
- NS: One dimensional array, containing the relative positions of the pseudosampling points.
- CE: One dimensional array, containing the nomalized experimental concentration data corresponding to NS.

A3. PROGRAM LISTING

```

1.0000 C      C(R,Z) CALCULATION.....
2.0000 C
3.0000      DIMENSION CA(15),CE(9),CMC(9),C(9),F(9,15),Z1(15),A(9),
4.0000      -          NS(9),R1(15),R2(15),V(15),W(9),WO(15),WS(9)
5.0000      DATA (Z1(I),I=1,8)/0.987993,0.937273,0.848207,0.724418,
6.0000      -          0.570972,0.394151,0.201194,0.000000/
7.0000      DATA (WO(I),I=1,8)/0.030753,0.070366,0.107159,0.139571,
8.0000      -          0.166269,0.186161,0.198431,0.202578/
9.0000      DATA NR,NF,NW/15,50,6/
10.0000     DATA B,Q/1.0,0.0/
11.0000 C
12.0000 C      DATA---TO BE UPDATED.....
13.0000 C
14.0000     DATA ND,TR,TZ,TEM,D,VA,BK,WK/
15.0000     -6,0.2,45,0,881,0,2.26,102,0,2.66,0.0570/
16.0000     DATA (NS(I),I=1,6)/
17.0000     -19,22,35,60,78,100/
18.0000     DATA (CE(I),I=1,6)/
19.0000     -0.75,0.71,0.60,0.44,0.35,0.24/
20.0000 C
21.0000 C      DATA---END.....
22.0000 C
23.0000     WRITE(2,800)
24.0000     WRITE(2,700)
25.0000     WRITE(2,300) TR,TZ
26.0000     WRITE(2,705)
27.0000     WRITE(2,300) TEM,VA
28.0000     WRITE(2,709)
29.0000     WRITE(2,300) D,BK,WK
30.0000     V0=2.0*VA
31.0000     AF=BK*TR*TR/(4.0*D)
32.0000     BT=WK*TR/(2.0*D)
33.0000     ZD=4.0*D/(V0*TR*TR)
34.0000     ZU=0.01*TZ*ZD
35.0000     WRITE(2,108)
36.0000     WRITE(2,350) AF,BT,ZD
37.0000     CALL EIGENV(AF,BT,W)
38.0000     NH=(NR+1)/2
39.0000     DO 5 I=1,NH
40.0000     J=NR-I+1
41.0000     R1(J)=(1.0+Z1(I))/2.0
42.0000     R2(I)=(1.0-Z1(I))/2.0
43.0000     WO(J)=WO(I)
44.0000 5     CONTINUE
45.0000     DO 10 I=1,NR
46.0000     R2(I)=R1(I)*R1(I)
47.0000 10    V(I)=V0*(1.0-R2(I))
48.0000     DO 20 M=1,NW
49.0000     WS(M)=SQRT(W(M))
50.0000 20    A(M)=0.5-(W(M)-AF)/(2.0*WS(M))

```

```

51.0000      WRITE(2,100)
52.0000      DO 30 M=1,NW
53.0000      FX=0.0
54.0000      FY=0.0
55.0000      DO 29 I=1,NR
56.0000      X=2.0*WS(M)*R2(I)
57.0000      CALL CHF(0,A(M),B,X,F(M,I),FS)
58.0000      T1=W0(I)*R1(I)*(1.0-R2(I))
59.0000      T2=EXP(-WS(M)*R2(I))*F(M,I)
60.0000      T=T1*T2
61.0000      FX=FX+T
62.0000 29    FY=FY+T*T2
63.0000      C(M)=FX/FY
64.0000 30    WRITE(2,200) M,W(M),C(M)
65.0000      WRITE(2,150)
66.0000      DO 35 L=1,ND
67.0000      ZX=ZU*NS(L)
68.0000      DO 36 I=1,NR
69.0000      CA(I)=0.0
70.0000      DO 37 M=1,NW
71.0000      WR=WS(M)*R2(I)
72.0000      WW=W(M)*ZX+WR
73.0000      IF(WW .GT. 100) GO TO 36
74.0000 37    CA(I)=CA(I)+C(M)*EXP(-WW)*F(M,I)
75.0000 36    CONTINUE
76.0000      VR=0.0
77.0000      CR=0.0
78.0000      DO 40 I=1,NR
79.0000      VD=W0(I)*R1(I)*V(I)
80.0000      CD=CA(I)*VD
81.0000      VR=VR+VD
82.0000 40    CR=CR+CD
83.0000      CMC(L)=CR/VR
84.0000      WRITE(2,200) NS(L),CE(L),CMC(L)
85.0000      Q=Q+(CMC(L)-CE(L))*(CMC(L)-CE(L))
86.0000 35    CONTINUE
87.0000      WRITE(2,500) Q
88.0000      STOP
89.0000 800   FORMAT(' ***** CUP-MIXING-CONC BY LAMINAR FLOW MODEL'
90.0000      -' *****',//)
91.0000 700   FORMAT(/,7X,'RADIUS(CM)',3X,'LENGTH(CM)')
92.0000 705   FORMAT(/,9X,'TEMP(*K)   VEL(CM/SEC)')
93.0000 709   FORMAT(/,5X,'D(CM*CM/SEC)   KB(1/SEC)   KW(CM/SEC)')
94.0000 200   FORMAT(10X,I3,7X,F9.4,6X,F9.4)
95.0000 100   FORMAT(/,11X,'NO.      EIGENVALUE   COEFFICIENT')
96.0000 108   FORMAT(/,12X,'ALPHA',8X,'BETA',4X,'LAMDA(1/CM)')
97.0000 150   FORMAT(/,6X,'DISTANCE(%)  EXPT(C/CO)   CALC(C/CO)')
98.0000 300   FORMAT(8X,F9.4,3X,F9.4,6X,F9.4)
99.0000 350   FORMAT(8X,F9.4,3X,F9.5,6X,F9.4)
100.0000 500  FORMAT(/,5X,'SUM OF SQUARES OF RESIDUALS IS',F9.6)
101.0000      END

```

```

102.0000 C   F(A,B,X) CALCULATION.....
103.0000 C
104.0000     SUBROUTINE CHF(KEY,A,B,X,F,FS)
105.0000     DATA NR,NF,NW/15,50,6/
106.0000     T=A/B*X
107.0000     F=1.0+T
108.0000     IF(KEY .EQ. 0) GO TO 20
109.0000     S=1.0/A
110.0000     FS=T*S
111.0000 20   DO 30 I=2,NF
112.0000     IF(ABS(T) .LT. 0.000001) RETURN
113.0000     J=I-1
114.0000     T=T*(A+J)/((B+J)*I)*X
115.0000     F=F+T
116.0000     IF(KEY .EQ. 0) GO TO 30
117.0000     S=S+1.0/(A+J)
118.0000     FS=FS+T*S
119.0000 30   CONTINUE
120.0000     RETURN
121.0000     END

```

```

122.0000 C      W CALCULATION,.....
123.0000 C
124.0000      SUBROUTINE EIGENV(AF,BT,W)
125.0000      DIMENSION W(9)
126.0000      DATA NR,NF,NW/15,50,6/
127.0000      DATA B,B1,B2/1.0,2.0,3.0/
128.0000      AB=AF+BT
129.0000      WI=2.0*AB-AB*AB/12.0+0.0001
130.0000      IF(BT .GT. 1.8284) WI=1.8284
131.0000      IF(AF .GT. 3) WI=AF
132.0000      DO 20 M=1,NW
133.0000 24      W0=WI
134.0000      KC=0
135.0000 25      CONTINUE
136.0000      WS=SQRT(W0)
137.0000      WR=1.0/WS
138.0000      X=2.0*WS
139.0000      WB=WS-BT
140.0000      WW=-(WS+AF*WR)/(4.0*W0)
141.0000      A=0.5-(W0-AF)/X
142.0000      A1=A+1.0
143.0000      A2=A1+1.0
144.0000      KC=KC+1
145.0000      CALL CHF(1,A,B,X,F0,FS0)
146.0000      CALL CHF(1,A1,B1,X,F1,FS1)
147.0000      CALL CHF(0,A2,B2,X,F2,FS2)
148.0000      F=WB*F0-A*X*F1
149.0000      DF1=0.5*WR*F0+WB*(A/B*WR*F1+WW*FS0)
150.0000      DF2=(A*WR+X*WW)*F1+A*X*(A1/B1*WR*F2+WW*FS1)
151.0000      DF=DF1-DF2
152.0000      DW=-F/DF
153.0000      IF(M .EQ. 1) GO TO 29
154.0000      IF(DF/PW - 0.0) 29,29,28
155.0000 28      WI=WI*1.1
156.0000      GO TO 24
157.0000 29      AW=ABS(DW)
158.0000      W(M)=W0+DW
159.0000      IF(KC .GT. 10) GO TO 36
160.0000      IF(AW/W0 .LE. 0.001 .AND. ABS(F) .LE. 0.1) GO TO 36
161.0000      IF(W0 - 5.0) 30,30,31
162.0000 30      WM=0.5*W0
163.0000      GO TO 35
164.0000 31      WM=0.1*W0
165.0000 35      IF(AW - WM) 32,32,33
166.0000 32      W0=W(M)
167.0000      GO TO 25
168.0000 33      W0=W0+WM*AW/DW
169.0000      GO TO 25
170.0000 36      WI=W(M)*1.40+6.00
171.0000      PW=DF
172.0000 20      CONTINUE
173.0000      RETURN
174.0000      END

```

A4. COMPUTER OUTPUT

FASTFOR (CONVERSATIONAL VER 10)

***** CUP-MIXING-CONC BY LAMINAR FLOW MODEL *****

RADIUS(CM)	LENGTH(CM)	
0.2000	45.0000	
TEMP(*K)	VEL(CM/SEC)	
881.0000	102.0000	
D(CM*CM/SEC)	KB(1/SEC)	KW(CM/SEC)
2.2600	2.6600	0.0570
ALPHA	BETA	LAMDA(1/CM)
0.0118	0.00252	1.1078
NO.	EIGENVALUE	COEFFICIENT
1	0.0285	1.0044
2	6.4499	-0.0058
3	20.9964	0.0021
4	43.5732	-0.0011
5	74.1662	0.0007
6	112.7695	-0.0005
DISTANCE(%)	EXPT(C/C0)	CALC(C/C0)
19	0.7500	0.7633
22	0.7100	0.7314
35	0.6000	0.6080
60	0.4400	0.4261
78	0.3500	0.3299
100	0.2400	0.2413

SUM OF SQUARES OF RESIDUALS IS 0.001297

B. RESPONSE SURFACE METHOD FOR k_b & k_w ESTIMATIONS

B1. GENERAL GUIDES

This program calculates the optimum k_b and k_w values. It is good for on-line operating only. The initial values of k_b and k_w is read for each cycle of determination of a pair of optimum k_b and k_w during the execution of the program.

The magnitudes of CRIT1 and CRIT2 depend on the goodness of experimental data as well as on the desired accuracy of the rate constants. Accordingly, it may be required to adjust the constants, 1.5 [77] and 8.0 [115].

Note: The number in [] stands for the statement number in the program.

B2. IDENTIFICATION VARIABLES IN DATA BOLCK

- CRIT1: Criterion to stop the procedure of modifying the initial values of k_b and k_w .
- CRIT2: Criterion to stop the programming.
- N: Number of experimental data.
- TR: Reactor diameter, cm.
- TZ: Reactor length, cm.
- VA: Minimum of average velocities, cm/sec.
- DC: Binary diffusion coefficient, cm^2/sec .
- NBS: One Dimensional array, containing the relative positions of pseudosampling points (to their very previous points).
- CE: One dimensional array, containing the nomalized experimental concentration data corresponding to NBS.

B3. PROGRAM LISTING

```

1.0000 C   RESPONSE SURFACE METHOD FOR KB & KW ESTIMATIONS.....
2.0000 C
3.0000 C   NOTE : THIS PROGRAM IS GOOD FOR ON-LINE OPERATING ONLY
4.0000 C
5.0000 C   DIMENSION CE(8),X(2),P(2),Q(2,2),Y(2,2),
6.0000 C   --          CA(8),D(2),NBS(8),XM(2),T(2,2),QO(9)
7.0000 C   COMMON/OCT/CA,X,Q,QC,IE
8.0000 C   INTEGER YES,JUDGE
9.0000 C   DATA JUDGE,YES/'YES','YES'/
10.0000 C
11.0000 C   DATA---TO BE UPDATED.....
12.0000 C
13.0000 C   DATA CRIT1,CRIT2/0.07,0.001/
14.0000 C   DATA N,TR,TZ,VA,DC/
15.0000 C   -6,0.2,45.0,102.0,2.26/
16.0000 C   DATA (NBS(I),I=1,6)/
17.0000 C   -19,3,13,25,18,22/
18.0000 C   DATA (CE(I),I=1,6)/
19.0000 C   -0.75,0.71,0.60,0.44,0.35,0.24/
20.0000 C
21.0000 C   DATA---END.....
22.0000 C
23.0000 C   MAIN PROGRAM
24.0000 C
25.0000 C   WRITE(2,500)
26.0000 C   WRITE(2,101)
27.0000 C   WRITE(2,102) TR
28.0000 C   WRITE(2,103) TZ
29.0000 C   WRITE(2,104) VA
30.0000 C   WRITE(2,105) DC
31.0000 C   WRITE(2,106)
32.0000 C
33.0000 C   IE=TIMES OF FUNCTIONAL EQUATION; IP=RUNS OF PAIR
34.0000 C
35.0000 C   IP=0
36.0000 C
37.0000 C 1001 IE=0
38.0000 C   IP=IP+1
39.0000 C   WRITE(2,107) IP
40.0000 C   READ(1,*) X(1),X(2)
41.0000 C
42.0000 C   IT=STEPS; IN=FIRST EXPLORATION; ID=IMPROVEMENT; IU=FAIL
43.0000 C
44.0000 C   IT=3
45.0000 C   IN=0
46.0000 C   ID=0
47.0000 C   IU=1
48.0000 C

```

```
49.0000 C      SECTION ONE.....A BETTER START
50.0000 C
51.0000      WRITE(2,125)
52.0000      WRITE(2,150)
53.0000 1      CALL SIMUL(N,NBS,TR,TZ,VA,CE,CA,X(1),X(2),DC,QM)
54.0000      IE=IE+1
55.0000      WRITE(2,155) X(1),X(2),QM
56.0000      IF(QM-CRIT1*N) 5,2,2
57.0000 2      CAL=0.0
58.0000      EXP=0.0
59.0000      DO 3 I=1,N
60.0000      CAL=CAL+CA(I)
61.0000      EXP=EXP+CE(I)
62.0000 3      CONTINUE
63.0000      IF(CAL .LT. EXP) GO TO 4
64.0000      X(1)=X(1)*1.25
65.0000      X(2)=X(2)*1.25
66.0000      GO TO 1
67.0000 4      X(1)=X(1)*0.8
68.0000      X(2)=X(2)*0.8
69.0000      GO TO 1
70.0000 C
```

```

71.0000 C SECTION TWO.....CALCULATION OF DIRECTION
72.0000 C
73.0000 5 CONTINUE
74.0000 C
75.0000 C SI=STEP SIZE
76.0000 C
77.0000 SI=1.5*SQRT(QM)*0.05
78.0000 QC=QM
79.0000 DO 9 L=1,2
80.0000 Y(L,1)=X(L)*(1.0-SI)
81.0000 Y(L,2)=X(L)*(1.0+SI)
82.0000 9 CONTINUE
83.0000 WRITE(2,135)
84.0000 WRITE(2,150)
85.0000 DO 19 I=1,2
86.0000 DO 19 J=1,2
87.0000 F(1)=Y(1,I)
88.0000 F(2)=Y(2,J)
89.0000 CALL SIMUL(N,NBS,TR,TZ,VA,CE,CA,F(1),F(2),DC,Q(I,J))
90.0000 IE=IE+1
91.0000 WRITE(2,155) F(1),F(2),Q(I,J)
92.0000 IF(Q(I,J) .LT. QC) ID=1
93.0000 19 CONTINUE
94.0000 IF(QC .LT. (CRIT2*N)) GO TO 21
95.0000 IF(ID .EQ. 1) GO TO 27
96.0000 21 WRITE(2,300)
97.0000 READ(1,100) JUDGE
98.0000 IF(JUDGE .NE. YES) GO TO 9999
99.0000 IF(IU .NE. 0) GO TO 27
100.0000 PI=PI*2.0-1.0
101.0000 GO TO 49
102.0000 27 ID=0
103.0000 DO 29 L=1,2
104.0000 DO 29 I=1,2
105.0000 T(L,I)=0.0
106.0000 29 CONTINUE
107.0000 DO 39 I=1,2
108.0000 DO 39 K=1,2
109.0000 T(1,K)=T(1,K)+Q(K,I)
110.0000 T(2,K)=T(2,K)+Q(I,K)
111.0000 39 CONTINUE
112.0000 BASE=ABS(T(2,1)-T(2,2))
113.0000 IF(BASE .LE. 0.000001) BASE=ABS(T(1,1)-T(1,2))
114.0000 DO 45 L=1,2
115.0000 D(L)=8.0*(T(L,1)-T(L,2))/BASE*SI*X(L)
116.0000 45 CONTINUE
117.0000 C

```

```

118.0000 C      SECTION THREE.....GOAL
119.0000 C
120.0000 C      PI=PARTITION; IU=FAIL; IS=SIGN
121.0000 C
122.0000      PI=1.0
123.0000      IU=0
124.0000 49     IS=1
125.0000      WRITE(2,145)
126.0000      WRITE(2,150)
127.0000 C
128.0000 C      IB=IF BACKWARD; IG=TOTAL SUCCESS; IM=IF TOTAL SUCCESS
129.0000 C
130.0000 50     IB=0
131.0000 51     IG=1
132.0000 52     IM=0
133.0000      DO 59 I=1,IT
134.0000      DO 61 L=1,2
135.0000      F(L)=X(L)+D(L)*I/PI*IS
136.0000 61     CONTINUE
137.0000      CALL SIMUL(N,NBS,TR,TZ,VA,CE,CA,P(1),P(2),DC,QO(I))
138.0000      IE=IE+1
139.0000      WRITE(2,155) F(1),F(2),QO(I)
140.0000      IB=IB+1
141.0000      IF (QO(I) .GE. QM) GO TO 65
142.0000 62     ID=1
143.0000      IM=I
144.0000      QM=QO(I)
145.0000      DO 58 L=1,2
146.0000      XM(L)=F(L)
147.0000 58     CONTINUE
148.0000      GO TO 59
149.0000 65     IF(PI .GT. 2.0) GO TO 66
150.0000      IF(IN .EQ. 1) GO TO 66
151.0000 59     CONTINUE
152.0000      IN=1
153.0000 66     IF(IM .NE. IT) IG=0
154.0000      IF(ID .EQ. 0) GO TO 79
155.0000      IU=1
156.0000      ID=0
157.0000      DO 69 L=1,2
158.0000      X(L)=XM(L)
159.0000 69     CONTINUE
160.0000 79     IF(IG .EQ. 1) GO TO 52
161.0000      IF(PI .LE. 2.0) GO TO 89
162.0000      IF(IS .EQ. 1) GO TO 81
163.0000      IF(IU .EQ. 0) GO TO 21
164.0000      GO TO 5
165.0000 81     IF(IB .NE. 1) GO TO 5
166.0000      IS=-1
167.0000      GO TO 51
168.0000 89     PI=PI+FLOAT(IT*8)
169.0000      GO TO 50
170.0000 C

```

```

171.0000 9999 CALL OCTA(N,NBS,TR,TZ,VA,DC,CE)
172.0000 WRITE(2,305)
173.0000 READ(1,100) JUDGE
174.0000 IF(JUDGE .EQ. YES) GO TO 1001
175.0000 STOP
176.0000 100 FORMAT(A4)
177.0000 500 FORMAT(1X,20('*'),' RESPONSE SURFACE METHOD ',20('*'))
178.0000 101 FORMAT(///,20X,'*** OPERATING CONDITION ***')
179.0000 102 FORMAT(/,16X,' REACTOR: RADIUS: ',F6.2,' CM')
180.0000 103 FORMAT(32X,'LENGTH: ',F6.2,' CM')
181.0000 104 FORMAT(/,16X,' AVERAGE VELOCITY: ',F7.2,' CM/SEC')
182.0000 105 FORMAT(/,16X,' DIFFUSION COEFFICIENT:',F6.2,' CM/SEC')
183.0000 106 FORMAT(/,16X,' MESH NUMBER: 20 X 100')
184.0000 107 FORMAT(/' INITIAL GUESS FOR KB & KW:',25X,'PAIR:',I5)
185.0000 125 FORMAT(//,15X,'*** THE RESULTS ON A BETTER STARTING ',
186.0000 --'POINT ***')
187.0000 135 FORMAT(//,16X,'***** THE RESULTS ON THE SQUARE RUN',
188.0000 --' *****')
189.0000 145 FORMAT(//,20X,'*** THE RESULTS ON THE PROBE ***')
190.0000 150 FORMAT(/,16X,'KB',8X,'KW',9X,'SUM-SQUARE-RESIDUAL')
191.0000 155 FORMAT(14X,2(1X,F9.6),F13.8)
192.0000 160 FORMAT(' CUP-MIXING-CONC. DOWN THE REACTOR')
193.0000 300 FORMAT(//,' IS MORE ITERATION NEEDED? --- ',
194.0000 --'TYPE IN YES OR NO')
195.0000 305 FORMAT(//,' IS MORE PAIR OF KB & KW NEEDED? --- ',
196.0000 --'TYPE IN YES OR NO')
197.0000 END
198.0000 C

```

```

199.0000 C      SOLVING DIFFERENTIAL EQUATION BY CRANK-NICOLSON METHOD
200.0000 C
201.0000      SUBROUTINE SIMUL(N,NBS,TR,TZ,VA,CE,CMC,KB,KW,D,Q)
202.0000      DIMENSION C(21),R(21),V(21),RH(21),E(21),F(21),G(21),
203.0000      -      CE(N),CMC(N),NBS(N),Y(21),Z(21),CO(5)
204.0000      REAL KB,KW
205.0000      DATA CO/0.015556,0.071111,0.026667,0.071111,0.015556/
206.0000      DATA NR,NZ,N1/20,100,21/
207.0000      Q=0.0
208.0000      DZ=TZ/NZ
209.0000      DR=TR/NR
210.0000      R2=TR*TR
211.0000      DO 9 I=1,N1
212.0000      R(I)=FLOAT(I-1)/NR
213.0000      V(I)=2.0*VA*(1.0-R(I)*R(I))
214.0000      C(I)=1.0
215.0000 9      CONTINUE
216.0000      DL=2.0*D*DZ/(VA*R2)
217.0000      DR=DR/TR
218.0000      A=KB*R2/(4.0*D)
219.0000      B=KW*TR/(2.0*D)
220.0000      X=0.5/(DR*DR)
221.0000      X1=2.0*(X+A)
222.0000      DO 19 I=2,NR
223.0000      Y(I)=4.0*(1.0-R(I)*R(I))/DL
224.0000      Z(I)=1.0/(4.0*R(I)*DR)
225.0000      E(I)=Z(I)-X
226.0000      F(I)=Y(I)+X1
227.0000      G(I)=-Z(I)-X
228.0000 19      CONTINUE
229.0000      F(1)=2.0*X+2.0/DL+A
230.0000      G(1)=-2.0*X
231.0000      E(N1)=-2.0*X
232.0000      F(N1)=2.0*(X+B/DR+A)+B
233.0000      DO 69 M=1,N
234.0000      JP=NBS(M)
235.0000      DO 49 J=1,JP
236.0000      DO 39 I=2,NR
237.0000      RH(I)=-E(I)*C(I-1)+(Y(I)-X1)*C(I)-G(I)*C(I+1)
238.0000 39      CONTINUE
239.0000      RH(1)=(2.0/DL+G(1)-A)*C(1)-G(1)*C(2)
240.0000      RH(N1)=0.0
241.0000      CALL TRID (N1,E,F,G,C,RH)
242.0000 49      CONTINUE
243.0000      VR=0.0
244.0000      CR=0.0
245.0000      DO 59 MO=1,5
246.0000      L=(MO-1)*4
247.0000      DO 59 MI=1,5
248.0000      I=L+MI
249.0000      VD=CO(MI)*V(I)*R(I)
250.0000      CD=C(I)*VD
251.0000      VR=VR+VD
252.0000      CR=CR+CD
253.0000 59      CONTINUE
254.0000      CMC(M)=CR/VR
255.0000      Q=Q+(CMC(M)-CE(M))*2
256.0000 69      CONTINUE
257.0000      RETURN
258.0000      END
259.0000 C

```



```
260.0000 C      SOLVING DIFFERENCE EQUATIONS BY TRIDIAGONAL MATRIX
261.0000 C
262.0000      SUBROUTINE TRID (N,A,B,C,X,G)
263.0000      DIMENSION A(21),B(21),C(21),X(21),G(21),BB(21)
264.0000      DO 1 I=1,N
265.0000      BB(I)=B(I)
266.0000 1      CONTINUE
267.0000      DO 2 I=2,N
268.0000      T=A(I)/BB(I-1)
269.0000      BB(I)=BB(I)-C(I-1)*T
270.0000      G(I)=G(I)-G(I-1)*T
271.0000 2      CONTINUE
272.0000      X(N)=G(N)/BB(N)
273.0000      NI=N-1
274.0000      DO 3 I=1,NI
275.0000      J=N-I
276.0000      X(J)=(G(J)-C(J)*X(J+1))/BB(J)
277.0000 3      CONTINUE
278.0000      RETURN
279.0000      END
280.0000 C
```

```

281.0000 C      PRINT OUT SQUARE
282.0000 C
283.0000      SUBROUTINE OCTA(N,NBS,TR,TZ,VA,DC,CE)
284.0000      DIMENSION IW(2),Q(2,2),X(2),NBS(8),CE(8),CA(8)
285.0000      COMMON/OCT/CA,X,Q,QC,IE
286.0000      DATA IW/'EXPT','CALC'/
287.0000      WRITE(2,150)
288.0000      WRITE(2,175) IE
289.0000      WRITE(2,230)
290.0000      WRITE(2,235) (Q(I,2),I=1,2)
291.0000      DO 10 K=1,7
292.0000      WRITE(2,240)
293.0000 10     CONTINUE
294.0000      WRITE(2,202) QC
295.0000      DO 20 K=1,7
296.0000      WRITE(2,240)
297.0000 20     CONTINUE
298.0000      WRITE(2,236) (Q(I,1),I=1,2)
299.0000      WRITE(2,280) X(1),X(2)
300.0000      WRITE(2,285)
301.0000      WRITE(2,290) IW(1), (CE(I),I=1,N)
302.0000      CALL SIMUL(N,NBS,TR,TZ,VA,CE,CA,X(1),X(2),DC,QM)
303.0000      WRITE(2,290) IW(2), (CA(I),I=1,N)
304.0000      RETURN
305.0000 150    FORMAT(//,15X,'***** THE FINAL RESULTS ON THIS',
306.0000      -' PROGRAMMING *****',//)
307.0000 175    FORMAT(16X,'TOTAL EVALUATIONS OF FUNCTIONAL ',
308.0000      -' EQUATION:  'I3,//)
309.0000 202    FORMAT(25X,'I',9X,F10.8,8X,'I')
310.0000 230    FORMAT(/,25X,'KW',69X,'I')
311.0000 235    FORMAT(20X,'(,F10.8,')-----('F10.8,')')
312.0000 236    FORMAT(20X,'(,F10.8,')-----('F10.8,')-KB')
313.0000 240    FORMAT(25X,'I',27X,'I')
314.0000 280    FORMAT(//' THE SQUARE HAS KB =',F7.4,' KW =',F7.4,
315.0000      -' AS ITS CENTER')
316.0000 285    FORMAT(//,' THE CUP-MIXING-CONC. DOWN THE REACTOR')
317.0000 290    FORMAT(1X,A4,';',9F7.4,/,6X,9F7.4)
318.0000      END

```


*** THE RESULTS ON THE PROBE ***

KB	KW	SUM-SQUARE-RESIDUAL
0.631576	0.431959	0.09293395
0.607794	0.208558	0.02426628
0.584012	-0.014842	1.07051100
0.606843	0.199622	0.03210342
0.608745	0.217494	0.01765744
0.609697	0.226430	0.01229197
0.610648	0.235366	0.00817186
0.611599	0.244302	0.00512177
0.612550	0.253238	0.00304384
0.613502	0.262174	0.00187940
0.614453	0.271110	0.00167494
0.615404	0.280046	0.00243016

***** THE RESULTS ON THE SQUARE RUN *****

KB	KW	SUM-SQUARE-RESIDUAL
0.612567	0.270278	0.00158967
0.612567	0.271942	0.00161686
0.616339	0.270278	0.00164213
0.616339	0.271942	0.00171322

IS MORE ITERATION NEEDED ? --- TYPE IN YES OR NO
*YES

*** THE RESULTS ON THE PROBE ***

KB	KW	SUM-SQUARE-RESIDUAL
0.591603	0.264453	0.00173579
0.613539	0.270844	0.00159536
0.612625	0.270578	0.00159324
0.611711	0.270311	0.00158967
0.610797	0.270045	0.00158745
0.609883	0.269779	0.00158723
0.608969	0.269513	0.00159001

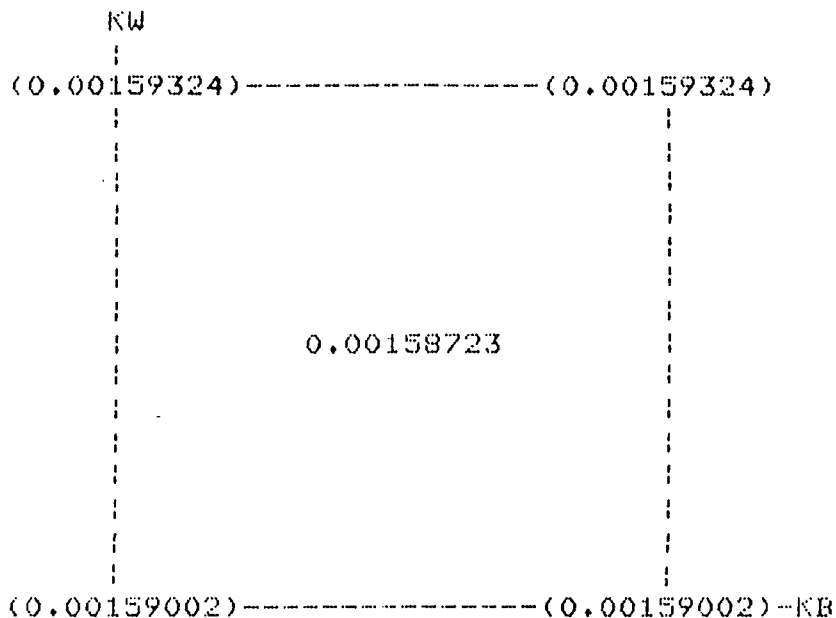
***** THE RESULTS ON THE SQUARE RUN *****

KB	KW	SUM-SQUARE-RESIDUAL
0.608061	0.268973	0.00159002
0.608061	0.270585	0.00159324
0.611705	0.268973	0.00159002
0.611705	0.270585	0.00159324

IS MORE ITERATION NEEDED ? --- TYPE IN YES OR NO
*NO

***** THE FINAL RESULTS ON THIS PROGRAMMING *****

TOTAL EVALUATIONS OF FUNCTIONAL EQUATION: 37



THE SQUARE HAS $KB = 0.6099$ $KW = 0.2698$ AS ITS CENTER

THE CUP-MIXING-CONC. DOWN-THE REACTOR

EXPT: 0.7500 0.7100 0.6000 0.4400 0.3500 0.2400

CALC: 0.7668 0.7347 0.6101 0.4266 0.3297 0.2406

IS MORE PAIR OF KB & KW NEEDED? --- TYPE IN YES OR NO
 *(CONTINUE TO OBTAIN THE SECOND PAIR OF OPTIMUM KB & KW VALUES)

APPENDIX 6 MECHANISTIC ANALYSIS

The mechanism of the pyrolysis of 1,1,1-trichloroethane in hydrogen at 881 °K was studied. The wall reaction was negligible at this temperature, and the reaction extent depended weakly on the diameter of a reactor. Fig. A2 shows the experimental distributions of major chlorinated hydrocarbon products. Table A3 outlines a general procedure for mechanistic modeling analysis. Table A4 illustrates the results from this preliminary mechanistic analysis. It is noted that this is only an initial-first try at modeling this reaction system and further mechanistic modeling, with more accurate rate constants, will undoubtedly lead to better fits to the experimental data.

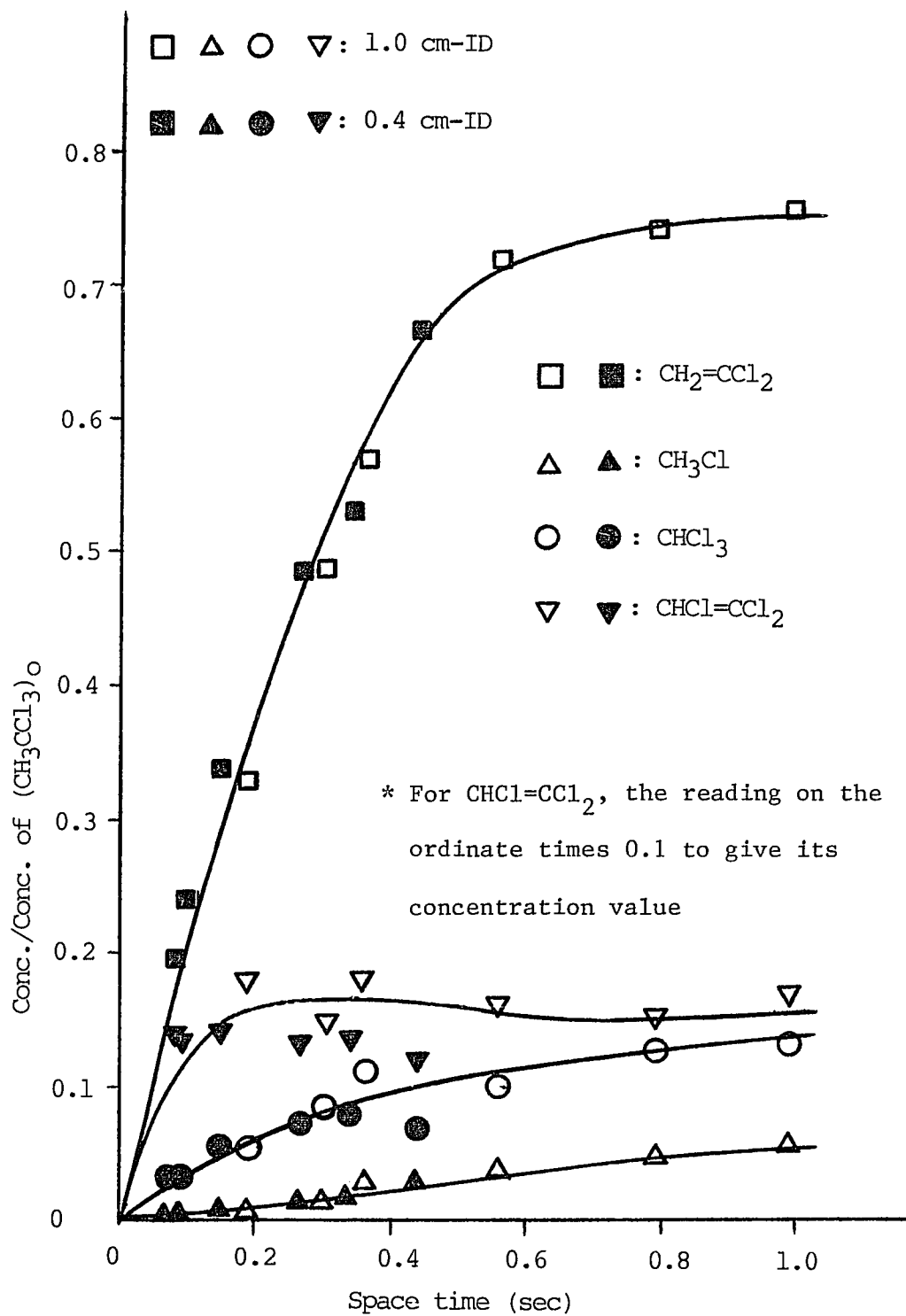


Fig. A2: Experimental distributions of major chlorinated hydrocarbon products.

Table A3: Procedure for mechanism study

1. Set up as many probable elementary reactions as possible from the experimentally obtained product distributions and from consideration of similar combustion chemistry.

2. Obtain the values of equilibrium constants, and rate constants from literature, by theoretical calculations (Benson, 1976), or by comparison to similar reactions.

3. Set up the rate equation for each component.

4.* Perform mechanism reduction and quasi-steady-state approximation by sensitivity analysis (Hwang, Dougherty, Rabitz, and Rabitz, 1978)/Principal Component Analysis (Vajda, Valko, and Turanyi, 1985).

5. Integrate the rate equations by STINT integrator (Tandler, Bickart and Picel, 1978) to obtain the concentration profiles.

6.* Adjust the values of those rate constants which are most questionable by optimization technique.

7. Return to Step 1 if necessary.

* Not yet done.

Table A4: Calculated major product distributions of the pyrolysis of CH_3CCl_3 in H_2 .

Product	Time (sec)				
	$3.05(-5)^a$	$6.10(-5)$	$1.22(-4)$	$2.44(-4)$	$4.88(-4)$
H_2	$1.00(0)^b$	$9.99(-1)$	$9.98(-1)$	$9.93(-1)$	$9.74(-1)$
CH_3CCl_3	$6.65(-2)$	$6.61(-2)$	$6.47(-2)$	$5.94(-2)$	$4.04(-2)$
HCl	$2.06(-4)$	$6.08(-4)$	$2.02(-3)$	$7.31(-3)$	$2.63(-2)$
CH_3CHCl_2	$1.85(-4)$	$5.70(-4)$	$1.95(-3)$	$7.18(-3)$	$2.60(-2)$
$\text{CH}_2=\text{CCl}_2$	$1.96(-6)$	$3.55(-6)$	$6.70(-6)$	$1.27(-5)$	$2.24(-5)$
$\cdot\text{CCl}_2\text{CH}_3$	$1.90(-5)$	$3.44(-5)$	$6.49(-5)$	$1.23(-4)$	$2.16(-4)$
$\cdot\text{CH}_2\text{CCl}_3$	$2.71(-9)$	$5.03(-9)$	$9.03(-9)$	$1.70(-8)$	$2.97(-8)$
$\text{H}\cdot$	$4.8(-11)$	$9.0(-11)$	$1.6(-10)$	$3.4(-10)$	$8.4(-10)$

- a. Numbers in parentheses indicate powers of ten.
- b. Concentration was normalized, based on $[\text{H}_2]_0$.
- c. Integration stopped at 4.88×10^{-4} sec because of the failure in the convergence test.

Table A5: Calculated rate constants at 881 °K for the elementary reactions considered in the pyrolysis of CH_3CCl_3 in H_2 .

Reaction	Rate constant ^a	
	Forward	Reverse
$\text{CH}_3\text{CCl}_3 \rightleftharpoons \text{CH}_2=\text{CCl}_2 + \text{HCl}$	7.88 (-1) ^b	4.89 (-4)
$\text{CH}_3\text{CCl}_3 \rightleftharpoons \cdot\text{CCl}_2\text{CH}_3 + \text{Cl}\cdot$	3.82 (0)	1.86 (12)
$\text{Cl}\cdot + \text{H}_2 \rightleftharpoons \text{HCl} + \text{H}\cdot$	2.32 (15) ^c	2.36 (15)
$\text{CH}_3\text{CCl}_3 + \text{H}\cdot \rightleftharpoons \cdot\text{CH}_2\text{CCl}_3 + \text{H}_2$	3.51 (12)	4.19 (9)
$\text{CH}_3\text{CCl}_3 + \text{H}\cdot \rightleftharpoons \cdot\text{CCl}_2\text{CH}_3 + \text{HCl}$	2.81 (12)	3.60 (1)
$\cdot\text{CCl}_2\text{CH}_3 + \text{H}_2 \rightleftharpoons \text{CH}_3\text{CHCl}_2 + \text{H}\cdot$	4.56 (5)	7.37 (9)
$\cdot\text{CH}_2\text{CCl}_3 + \text{Cl}\cdot \rightleftharpoons \text{CH}_2\text{ClCCl}_3$	2.20 (6)	1.75 (2)
$\text{CH}_2\text{ClCCl}_3 \rightleftharpoons \text{CHCl}=\text{CCl}_2 + \text{HCl}$	8.97 (0)	2.57 (-1)
$\text{CH}_2\text{ClCCl}_3 \rightleftharpoons \cdot\text{CH}_2\text{Cl} + \cdot\text{CCl}_3$	1.86 (-16)	3.92 (-3)
$\cdot\text{CH}_2\text{Cl} + \text{H}_2 \rightleftharpoons \text{CH}_3\text{Cl} + \text{H}\cdot$	4.59 (8)	2.04 (10)
$\cdot\text{CCl}_3 + \text{H}_2 \rightleftharpoons \text{CHCl}_3 + \text{H}\cdot$	1.61 (7)	1.64 (10)
$\text{Cl}\cdot + \text{H}\cdot \rightleftharpoons \text{HCl}$	1.00 (15)	2.64 (-7)
$2\text{H}\cdot \rightleftharpoons \text{H}_2$	1.00 (15)	2.69 (-7)

- a. Rate constants are expressed in the units of a suitable combination of mole, liter, and second.
- b. numbers in the parentheses indicate powers of ten.
- c. From Benson, S.W, F.R. Cruickshank, and R. Shaw, *Int. J. Chem. Kinet.*, 1, 29 (1969).

SELECTED BIBLIOGRAPHY

- * Barton, D.H.R., and P.F. Onyon, J. Am. Chem. Soc. 72, 988 (1950).
- * Benson, S.W., and G.N. Spokes, Symp. Combust. 1966, 11, 95 (Pub. 1967).
- * Benson, S.W., "Thermochemical Kinetics", John Wiley & Sons, New York, NY, (1976).
- * Bird, R.B., W.E. Stewart, and E.N. Lightfoot, "Transport Phenomena", John Wiley & Sons, New York, NY, Chap. 20 (1960).
- * Black, G., H. Wise, S. Schechter, and R.L. Sharpless, J. Chem. Phys., 60 (9), 3526 (1974).
- * Box, G.E.P., and K.B. Wilson, J. Roy. Soc., Ser[B(13), 1 (1951)].
- * Box, G.E.P., W.G. Hunter, and J.S. Hunter, "Statistics for Experimenters", John Wiley & Sons, New York, NY, Chap. 15 (1978).
- * Chuang, S. C., M.S. Thesis, New Jersey Institute of Technology, Newark, NJ, (1982).
- * Cleland, F.A., and R.H. Wilhelm, AIChE, 2, 489 (1956).
- * Cvetanović, R.J., D.L. Singleton, and G. Parakevopoulos, J. Phys. Chem., 83(1), 50 (1979).
- * Froment, G.F., and K.B. Bischoff, "Chemical Reactor Analysis and Design", John Wiley & Sons, New York, NY, Chap. 9 (1979).

- * Fuller, E.N., P.D. Schettler, and J.C. Giddings, Ind. Eng. Chem. 58(5), 19 (1966).
- * Howard, C.J., J. Phys. Chem. 83 (1), 3 (1979).
- * Hwang, J.T., E.P. Dougherty, and J. Rabitz, J. Chem. Phys. 69 (11), 5180 (1978).
- * Kaufman, F. in "Progress in Reaction Kinetics", G. Porter edited, Pergamon Press, New York, NY, Vol. 1, 1 (1961).
- * Lapidus, Leon, "Digital Computation for Chemical Engineers", McGraw-Hill Book Company, New York, NY, Chap. 4 (1962).
- * Lauwerier, H.A., Appli. Sci. Res., A8, 366 (1959).
- * Levenspiel, Octave, "Chemical reaction Engineering", 2nd. ed., John Wiley & Sons, New York, NY, Chap. 3/9 (1972).
- * Mahmood, B., M.S. Thesis, New Jersey Institute of Technology, Newark, NJ (1985).
- * Marrero, T.R., and E.A. Mason, AIChE J. 19 (3), 498 (1973).
- * Mulcahy, M.F.R., "Gas Kinetics", John Wiley & Sons, New York, NY, Chaps. 3/4 (1973).
- * Nain V.P.S, and J.R. Ferron, Ind. Eng. Chem. Fundam., 11 (3) 420 (1972).
- * Ogren, P.J., J. Phys. Chem. 79(17), 1749 (1975).
- * Poirier, R.W., and R.J. Carr, J. Phys. Chem., 75, 1593 (1971).

- * Reid, R.C., J.M. Prausnitz, and T.K. Sherwood, "The Properties of Gases and Liquids", 3rd. ed., McGraw-Hill Book Co., New York, NY (1976).
- * Slater, L.J., "Confluent Hypergeometric Functions", Cambridge U.P., Cambridge, Chap. 5 (1960).
- * Smith, G.K., B.B. Krieger, and P.M. Herzog, AICHE J. 26 (4), 567 (1980).
- * Tendler, J.M., T.A. Bickart, and Z. Picel, ACM Trans. Math. Software, 4 (4), 339 (1978).
- * Vajda, S., P. Valko, and T. Turanyi, Int. J. Chem. Kinet., 17, 55 (1985).
- * Weast, R.C., "CRC Handbook of Chemistry and Physics", 63rd. ed., CRC Press, Inc., Boca Raton, Fl., D-204 (1982).
- * Wissler, E.H., and R.S. Schechter, Appl. Sci., Res., A10, 198 (1961).